

# UNIVERSITY OF VERONA



**Department of**  
Diagnostics and Public Health

**PhD School of**  
Natural Sciences and Engineering

**PhD in**  
Nanoscience and Advanced Technologies  
XXXIV cycle (2018)

**PAPER-BASED MICROFLUIDIC DEVICES FOR FORENSIC SCIENCES: DEVELOPMENT AND  
VALIDATION OF INNOVATIVE TOOLS**

**S.S.D. MED/43**

**Coordinator:** Prof. Adolfo Speghini

**Tutor:** Prof. Franco Tagliaro

**PhD Student:** Yvane Agard

YEAR 2021

UNIVERSITA' DEGLI STUDI DI VERONA

DEPARTMENT OF  
DIAGNOSTICS AND PUBLIC HEALTH

DOCTORAL SCHOOL  
NATURAL SCIENCES AND ENGINEERING  
DOCTORAL PROGRAM IN  
NANOSCIENCE AND ADVANCED TECHNOLOGIES

WITH THE FINANCIAL CONTRIBUTION OF  
FONDAZIONE CARIVERONA

University of Verona

Cycle / year 34 / 2018

TITLE OF THE DOCTORAL THESIS

PAPER-BASED MICROFLUIDIC DEVICES APPLIED TO FORENSIC SCIENCES:  
DEVELOPMENT AND VALIDATION OF INNOVATIVE TOOLS

S.S.D. MED/43

Coordinator: Prof. Adolfo Speghini

Signature 

Tutor: Prof. Franco Tagliaro

Signature 

Doctoral Student: Dott.ssa Yvane Agard

Signature 

\* For the list of S.S.D. please refer to the Ministerial Decree of 4<sup>th</sup> October 2000, Attachment A "Elenco dei Settori Scientifico – Disciplinari" available at: [http://www.miur.it/atti/2000/alladm001004\\_01.htm](http://www.miur.it/atti/2000/alladm001004_01.htm)

*To my mummy, Yvonne Agard, the symbolism and content of this PhD are dedicated to you. For your sacrifice, your vision, your love, your perseverance. The best parts of me are from you- your confidence, humility, tenacity, I thank you for it all. I am so grateful that God chose you as the portal.*

*To my Addie, this love I have experienced with you has healed, changed and brought out the best in me. I am so excited to do life with you. I thank God constantly for the presence of you in my life.*

*And finally, to my Aunty Yvonne, the author of so many of my memories, I love and miss you so much. Thank you for your eternal guidance. This PhD is ultimately the actualisation of your dream of me being Dr Yvane Agard.*

*I love you all, with all of me...*

## **Table Of Contents**

<b>1. FRAMEWORK AND AIMS .....</b>	<b>5</b>
<b>2. INTRODUCTION .....</b>	<b>7</b>
<b>2.1 ASSURED Criteria .....</b>	<b>7</b>
<b>2.2 <math>\mu</math>PADs in Forensic Science .....</b>	<b>9</b>
<b>2.2 Microfluidics .....</b>	<b>9</b>
<b>2.3 Paper .....</b>	<b>10</b>
2.3.1 Why Paper? .....	10
2.3.2 Paper surface and its Modification .....	10
<b>2.4 Fabrication Methods .....</b>	<b>12</b>
2.4.1 Wax Printing .....	13
2.4.2 Sol-gel .....	14
<b>2.5 Detection .....</b>	<b>15</b>
2.5.1 Colorimetry .....	16
2.5.2 Hyphenated Detection Methods .....	16
<b>3. ESTIMATION OF TIME SINCE DEATH: ASSESSMENT OF POINT-OF-NEED DEVICES FOR DETERMINATION OF AMMONIUM CONCENTRATION IN THE VITREOUS HUMOUR .....</b>	<b>17</b>
<b>3.1 Introduction .....</b>	<b>17</b>
<b>3.2 Materials and Methods.....</b>	<b>19</b>
3.2.1 Chemicals.....	19
3.2.2 Sample collection.....	19
3.2.3 Direct Mixing.....	19
3.2.4 Gas diffusion device.....	19
3.2.5 Fabrication of $\mu$ PAD .....	20
Analysis of samples .....	21
3.2.6 Validation.....	21
<b>3.3 Results and Discussion .....</b>	<b>22</b>
3.3.1 Optimisation studies for gas diffusion device .....	24
3.3.2 Preliminary assessment of the suitability of the Nessler's reagent for the analysis of VH (Direct mixing study) .....	26
3.3.3. Design and validation of the microfluidic paper-based device and gas diffusion device .....	28
3.3.4 Method validation .....	30
3.3.5 Analysis of real samples.....	32
3.3.6 Overall comparison of three investigated methods .....	36
<b>3.4 Conclusion .....</b>	<b>37</b>
<b>3.5 Future research .....</b>	<b>37</b>
<b>4. THE DEVELOPMENT OF A PAPER-BASED MICROFLUIDIC DEVICE AS A PRELIMINARY SCREENING TEST FOR DRUGS OF ABUSE IN URINE: DETERMINATION OF CONCENTRATION OF URINARY CREATININE .....</b>	<b>38</b>
<b>4.1 Introduction .....</b>	<b>38</b>

<b>4.2 Materials and Methods</b> .....	<b>40</b>
4.2.1 Chemicals.....	40
4.2.2 Fabrication of $\mu$ PAD.....	40
4.2.3 Analysis of samples.....	41
4.2.4 Validation.....	41
<b>4.3 Results and Discussion</b> .....	<b>42</b>
4.3.1 Design and validation of the microfluidic paper-based device.....	44
4.3.2 Optimisation studies.....	47
4.3.3 Analysis of real samples.....	48
<b>4.4 Conclusion</b> .....	<b>50</b>
<b>4.5 Future research</b> .....	<b>51</b>
<b>5. THE DEVELOPMENT OF A PAPER-BASED MICROFLUIDIC DEVICE CAPABLE OF CONDUCTING RECOMBINASE POLYMERASE AMPLIFICATION (RPA) FOR THE DETECTION OF CARBAPENEMASES.</b> .....	<b>52</b>
<b>5.1 Materials and Methods</b> .....	<b>54</b>
5.1.1 Chemicals and Materials .....	55
5.1.2 Design and 3D printing of template unit.....	55
5.1.3 Fabrication of device.....	58
5.1.4 RPA on paper .....	58
<b>5.2 Results and Discussion</b> .....	<b>59</b>
5.2.1 Optimisation studies for sol gel and paper substrates.....	59
5.2.2 3D printed template.....	62
5.2.3 RPA studies.....	65
<b>5.3 Conclusion</b> .....	<b>67</b>
<b>5.4 Future work</b> .....	<b>68</b>
<b>6. ABBREVIATIONS</b> .....	<b>69</b>
<b>7. REFERENCES</b> .....	<b>73</b>
<b>8. APPENDICES</b> .....	<b>77</b>
<b>8.1 Appendix I. <math>\text{NH}_4^+</math> in vitreous humour</b> .....	<b>77</b>
8.1.1 List of vitreous humour samples used in the study .....	77
8.1.2 Reproducibility studies for GD and $\mu$ PAD methods .....	78
<b>8.2 Appendix II. Creatinine in urine</b> .....	<b>80</b>
8.2.1 List of urine samples used in the study .....	80
8.2.2 Reproducibility studies for the reagents used in the study .....	81
<b>8.3 Appendix III. RPA Studies</b> .....	<b>84</b>
8.3.1 Schematic of Recombinase Polymerase Amplification.....	84
8.3.2 Full list of Chemicals .....	84
8.3.3 Functionalising/ Priming of Magnetic beads with VIM Biotinylated Forward primer .....	85
8.3.4 Components of RPA mixture .....	85
8.3.5 Results of RPA studies.....	86
<b>9. ACKNOWLEDGEMENTS</b> .....	<b>87</b>

## **TABLE OF FIGURES**

Fig. 2.1 Summary of ASSURED criteria.....	8
Fig. 2.2 The chemical structure of the polysaccharide, cellulose. ....	11
Figure 2.3. Schematic of patterning paper using photolithography.....	13
Fig. 2.4 Example of colorimetric detection.....	15
Fig. 3.1 Schematic of gas diffusion device. ....	20
Fig. 3.2 Schematic of $\mu$ PAD used in the determination of ammonium concentrations in vitreous humour samples. ....	21
Fig. 3.3 Evaluation of best dilution of Nessler's reagent. ....	24
Fig. 3.4. The estimation of the best time interval to record image. ....	25
Fig. 3.5 Linearity and specificity studies for direct mixing method .....	28
Fig 3.6 Effect of temperature and storage on RGB distance .....	29
Fig. 3.7 Linearity and corresponding images of GD method.....	31
Fig. 3.8 Linearity and corresponding images of $\mu$ PAD method.....	32
Fig. 3.9 Specificity studies for $\mu$ PAD method.....	32
Fig 3.10: Correlation between CE-UV and $\mu$ PAD method .....	33
Fig 3.11: Correlation between CE-UV and GD method .....	34
Fig 3.12: Correlation between PMI and $[\text{NH}_4^+]$ from $\mu$ PAD method.....	35
Fig 3.13: Correlation between PMI and $[\text{NH}_4^+]$ from GD method.....	35
Fig 4.1 Schematic of origami $\mu$ PAD.....	40
Fig 4.2 Reaction of creatinine and picric acid in NaOH resulting in characteristic yellow chromogen. ....	43
Fig 4.3 Reaction of creatinine and 3,5-dinitrobenzoic acid in NaOH resulting in characteristic purple chromogen.....	43
Fig 4.4 Reaction of creatinine and Nessler's reagent in NaOH resulting in yellow brown colour. ....	44
Fig. 4.5 Linearity and optical images of increasing creatinine concentration interaction with Nessler's reagent.....	45
Fig. 4.6 Linearity and optical images of increasing creatinine concentration interaction with picric acid solution.....	46
Fig. 4.7 Linearity and optical images of increasing creatinine concentration interaction with DNBA solution .....	46
Fig 4.8 Specificity studies.....	47
Fig. 4.9 Correlation between immunoassay and $\mu$ PAD method .....	49
Fig. 4.10 Correlation between immunoassay and RGB distance.....	50
Figure 5.1: Schematic diagram of magnetic beads application to extract target analytes.....	54
Fig. 5.2 Illustration of template.....	55
Fig. 5.3 PrusaSlicer images of components of template unit.....	57

Fig. 5.4 Schematic of resultant paper-based microfluidic device .....	58
Fig 5.5 Results of sol gel impregnation studies .....	61
Figure 5.6 Images of components of 3D printed template unit.....	63
Figure 8.1 Schematic of Recombinase polymerase amplification. ....	84

## LIST OF TABLES

*Table 3.1: Summary of parameters investigated to achieve the optimal analysis conditions for gas diffusion device.*

*Table 3.2: Summary of parameters investigated to achieve the optimal analysis conditions for direct mixing analysis.*

*Table 3.3: Comparison of each method with ASSURED criteria*

*Table 5.1: Paper substrates evaluated for sol gel dipping with their corresponding polysaccharide type, pore size and charge.*

*Table 8.1: List of vitreous humour samples with the corresponding ammonium concentrations acquired for the CE-UV method as well as the determined concentrations using GD and  $\mu$ PAD methods.*

*Table 8.2: Reproducibility studies for  $\mu$ PAD method*

*Table 8.3: Reproducibility studies for GD method*

*Table 8.4: List of urine samples with the corresponding creatinine concentrations acquired for the immunoassay method as well as the determined concentrations using NR, PA and DNBA.*

*Table 8.5: Reproducibility studies for creatinine studies using NR*

*Table 8.6: Reproducibility studies for creatinine studies using PA*

*Table 8.7: Reproducibility studies for creatinine studies using DNBA*

*Table 8.8: Components and volumes of RPA mixture*

*Table 8.9: Results from RPA studies*

## 1. FRAMEWORK AND AIMS

Laboratory analyses usually require sophisticated equipment and skilled personnel. However, very often, the use of simplified procedures and techniques in various working conditions can prove useful in solving several problems. Forensic applications represent an emblematic example of this requirement to simplify and solve various difficulties. Legal medicine requires both highly sophisticated techniques to solve analytical problems and simple techniques with fast procedures that allow analyses to be carried out outside the laboratory, in remote areas by unqualified personnel. The implementation of paper-based microfluidic analytical devices ( $\mu$ PADs) for legal medicine presents an opportunity to tackle all the aforementioned limitations and requirements in the field of forensic science. It is also important to note that little to no sample preparation is required, with the ability to use many samples directly onto the  $\mu$ PADs for the analysis of the desired analyte.  $\mu$ PADs are very inexpensive to produce and can be produced in resource deficient and remote areas. They are rapid, require minute sample volumes, are easy to use and do not require skilled technicians.

The use of  $\mu$ PADs for various forensic science applications has been well investigated by many research groups with several other areas to explore [1]. To date, a wide range of drugs can be identified and/or quantified by  $\mu$ PADs. These include but not limited to, illicit drugs such as amphetamines, cocaine, morphine and codeine as well as the identification of substandard drugs, which usually occur when the amounts of active pharmaceutical ingredients (APIs) are altered in pharmaceutical drugs, in antibiotics and in herbal supplements which are not heavily regulated[2-5]. These devices have also been used for forensic serology, in the evaluation of gunshot residue and in the ground-breaking application of the estimated time of death by establishing the post-mortem interval, experiments which can all be performed at the scene of the crime [6-8]. In 2020, an innovative development in the implementation of  $\mu$ PADs in forensic science was achieved as Azuaje-Haulde et al developed a device with the ability to identify the Y human amelogenin gene, identifying male from female human specimen [9].  $\mu$ PADs have also shown utility in the identification of agents of warfare like explosives and chemical warfare agents like nerve agents, which can be instrumental for military intelligence

and defence whose aim is to acquire intel before, to protect civilians and after, to identify the components and if they are linked to a specific group or organization [10, 11].

Based on the application of these devices in other forensic contexts, the core of my research was the implementation of  $\mu$ PADs in forensic science aspects which required point-of-need platforms to be more beneficial to doctors, forensic scientists and investigators. This PhD thesis involves:

- The use of microfluidic devices to determine the estimated time since death.
- The development of a paper-based microfluidic device as a preliminary screening test for drugs of abuse in urine.

Additionally, as part of my research period abroad, an emphasis was placed on exploring different fabrication methods to create devices that were resistant to more chemically aggressive assays. The final project discussed is:

- The development of a paper-based microfluidic device capable of conducting Recombinase Polymerase Amplification (RPA) for the detection of carbapenemases.

## 2. INTRODUCTION

Diagnostics play a critical role in healthcare and directly affects the treatment a patient receives, based on its accuracy. Over the years, great strides have been made in the development of advanced laboratory-based systems for the qualitative and quantitative analysis of various analytes. Although these have been revolutionary and allow for life-saving treatments and management of several diseases and ailments to be administered in a timely manner, the cost and complexity of the tests have also increased. This poses a problem for accessibility in resource-limited regions of the globe and ultimately infringes on two of the UN's Sustainable Development Goals, good health and well-being, and reduced inequalities. Efforts to develop alternative, more affordable methods were thus undertaken.

Although the initial need for alternatives to these intricate methods were spawned from their requirements in diagnostics, these solutions have applicability in several other fields including legal medicine.

Legal medicine or forensic science utilises many of these same complex equipment and procedures described and is closely related to diagnostics. The main difference is the reason for identifying and quantifying specific analytes. Where analysis in diagnostic medicine is to determine what is wrong with a patient, analysis in legal medicine establishes what transpired and who is at fault. Forensic medicine encompasses the administering of justice and ensuring the safety of the public.

### 2.1 ASSURED Criteria

In an effort to close the gap between the diagnostic privileges received in the developed world compared to the developing world, the WHO introduced a criterion, in 2003, as a guideline for the development of tests [12]. This was in turn also used in a forensic science context. The ASSURED (*Affordable, Sensitive, Specific User-friendly, Rapid and Robust, Equipment-free and Deliverable* to end users) criterion has been set as the benchmark and is followed by several researchers and programs in the development of their tests (Fig.2.1). More recently, environmental friendliness, real-time connectivity of devices, and scalability have been added as standards to supplement technological advancements.

Various difficulties lie in achieving every measure, as a requirement for greater sensitivity and specificity may incur greater costs and conversely, the development of an inexpensive, user-friendly device like lateral flow assays (LFAs) may lack specificity and sensitivity. Therefore, tests should not aim to completely replace laboratory instrumentation but rather, researchers should make an accurate evaluation of what the most important aspects of the ASSURED criteria are, for the test to be practicable and applicable in its specific setting.

In urban settings, with more resources and skilled personnel, sensitivity and specificity may be more easily achieved, whereas, in rural communities, equipment-free, easy-to-use, rapid tests are prioritised.

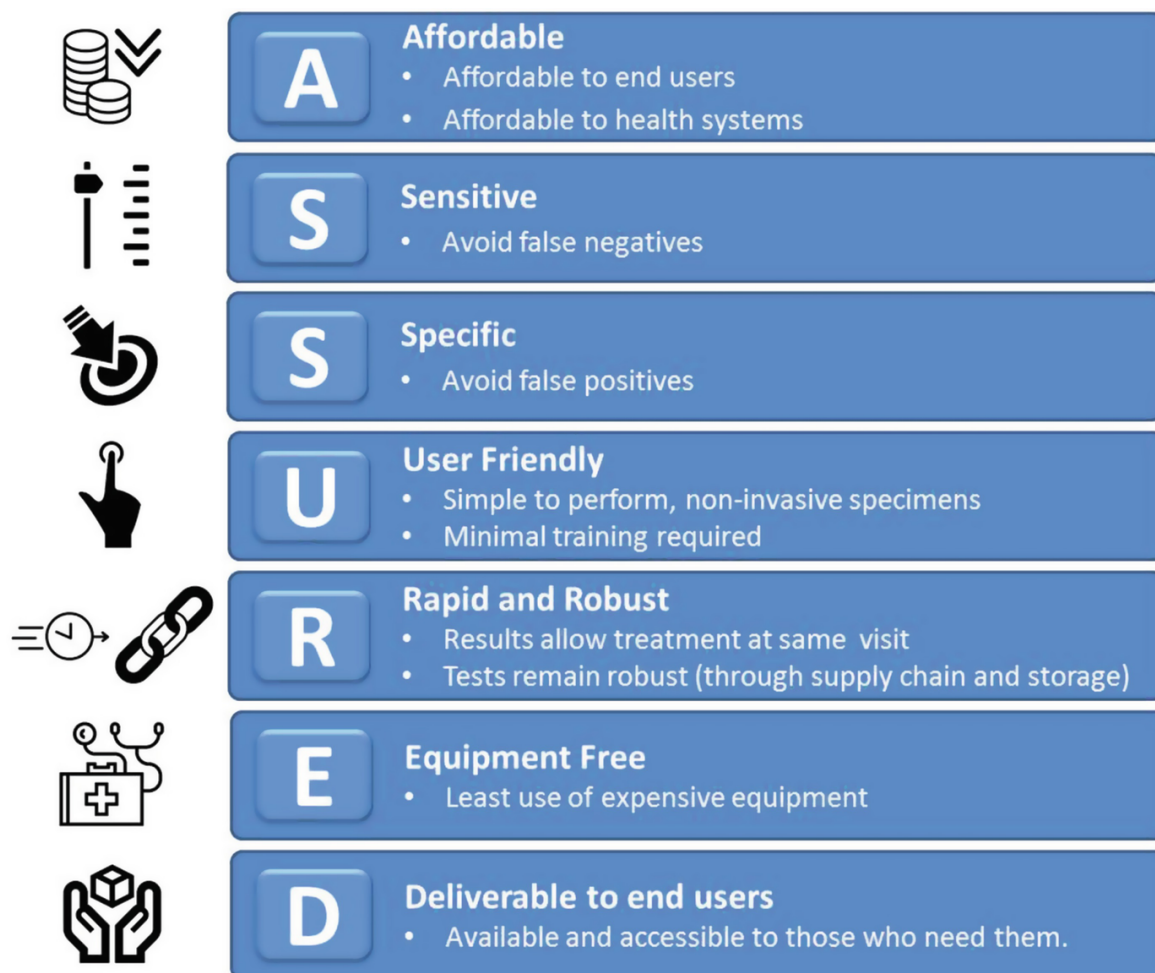


Fig. 2.1 Summary of ASSURED criteria as prescribed by the WHO. Reprinted (adapted) with permission from ref [13].

## 2.2 $\mu$ PADs in Forensic Science

Particularly in a forensic science setting, specific, rapid, equipment-free tests would be the most beneficial to crime scene investigators and/or medical personnel. Paper-based microfluidic analytical devices ( $\mu$ PADs) have shown great capacity as innovative analytical tools, which fulfil the ASSURED criteria, for the detection and quantification of analytes of interest.

The use of  $\mu$ PADs in forensic science ranges from the conventional perception of forensic science in relation to illicit and substandard drugs, both in biological samples as well as seized drugs to identification of fluids, the post-mortem interval and gunshot residue at crime scenes. Devices have also been developed to evaluate the more unconventional subdivisions of forensic science like identification of nerve agents used in war as well as chemical warfare agents. These devices which have been developed can be used as point-of-need devices or in the lab, replacing expensive instrumentation, as little to no sample treatment and minute volumes of samples are required. With biological samples, sample preparation is usually not required, with potentially only a dilution required. In the case where the analyte is an organic solid, for example in the case of illicit drugs, or an inorganic compound, for example in the case of gunshot residue, the solid is usually dissolved in an appropriate buffer solution or deionized water before the analysis.

The current work of several research groups has shown the variety of ways in which these easy to use, portable, low-cost devices can be employed, allowing for the envisioning of several more applications that have not yet been explored.

## 2.2 Microfluidics

Microfluidics is used to define both the science which studies the behaviour of fluids through micro-channels as well as the technology of manufacturing said devices. These devices are microminiaturised comprising chambers and channels through which fluids are confined and flow with the use of an external pump.

Traditionally, silicone derivatives, namely polydimethylsiloxane (PDMS) and silica, were used as the material for the fabrication of microfluidic devices [14]. However, in 2007, Martinez et

al revolutionised the field of microfluidics and its accessibility to unskilled workers in remote areas by the development of paper-based microfluidic analytical devices ( $\mu$ PADs) [15]. These devices comprise two areas- a hydrophobic region with a specific desired design, which serve as boundaries for the hydrophilic region where the analysis is conducted, on a paper support.

## 2.3 Paper

### 2.3.1 Why Paper?

Paper is low-cost, abundant, easily modified, biodegradable, easily disposed of and can be scaled to several billion devices a year.

Paper provides an interesting angle for the world of traditional microfluidics as it has the inherent ability for fluidic flow attained via capillary action without the need for pumps or external actuation. This is advantageous as the main goal of the development of paper-based devices is for their implementation in developing countries, in remote regions that may not have access to stable electricity if any at all [13].

### 2.3.2 Paper surface and its Modification

Paper is a bendable, foldable, porous solid due to the structure of its main component, cellulose. This porosity varies depending on the connectivity of its fibres, varying from a highly porous to a tight surface. Considering the diversity in its application and consequently the different modifications of its properties, it becomes apparent that there is no unique way to characterise its surface properties. In paper-based microfluidic devices the most common type of paper used is filter/ chromatographic paper due to its hydrophilicity, stability and sturdiness. The cellulose in paper fibres is primarily held together by hydrogen bonds in the dry state (Fig. 2.2). These bonds are relatively weak and so strengthening agents are added to enforce the bonds to ensure the mechanical strength when the paper is wet [16].

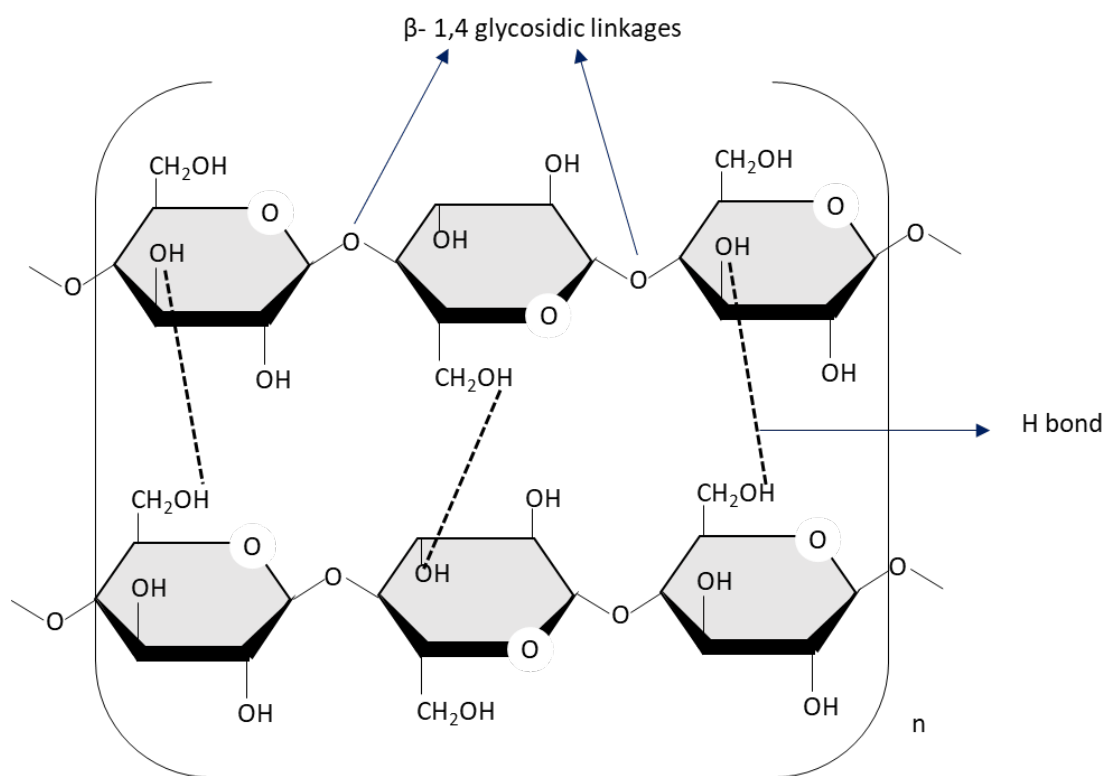


Fig. 2.2 The chemical structure of the polysaccharide, cellulose.

Each chain is held together by intramolecular H-bonds which attribute to the characteristics of cellulose

Current research and development indicate that power sources like batteries, screens for the visual display of results, biological materials, and many other functional features can be integrated into these paper-based devices by simply utilising various printing technologies and other manufacturing techniques which are readily available and well understood. The modification of the paper during manufacturing or in post-processing will allow for the alteration of chemical and physical properties of the paper to make it more suitable for specific reagents or reactions.

There is also the possibility to further modify the surface of the paper after its production. Examples of chemical modification of the paper surface include the addition of molecularly imprinted polymers, aptamers and hydrophobisation. Molecular imprinted polymers are used to increase selectivity and sensitivity of the desired analyte, usually a biological molecule, by the selective recognition of template molecules [17, 18]. Aptamers are single-stranded nucleic acids and are integrated into assays to bind to a target molecule with great affinity and specificity and are widely acknowledged as the nucleic acid counterpart of antibodies [19-21]. Hydrophobisation is the primary manner in which the paper surface of paper-based

microfluidic devices is modified as the formation of defined barriers by hydrophobisation is the distinguishing feature between  $\mu$ PADs and lateral flow assays (LFAs) [22]. All the fabrication techniques of  $\mu$ PADs involve hydrophobisation.

## 2.4 Fabrication Methods

In 2007, Whitesides' research group proposed the use of microfluidics paper-based devices as an alternative approach to the common point-of-care devices [15]. Although the original idea had already shown the potential for significantly impacting most scientific fields, the first developed  $\mu$ PADs fabricated by the photolithography process, was complicated with several steps (Fig 2.3). In order to overcome this limitation, several research groups proposed alternative fabrication methods, highlighted below are the fabrication methods used in the research.

The primary parameters to determine the success of each fabrication method are its ability for mass production and fast prototyping.

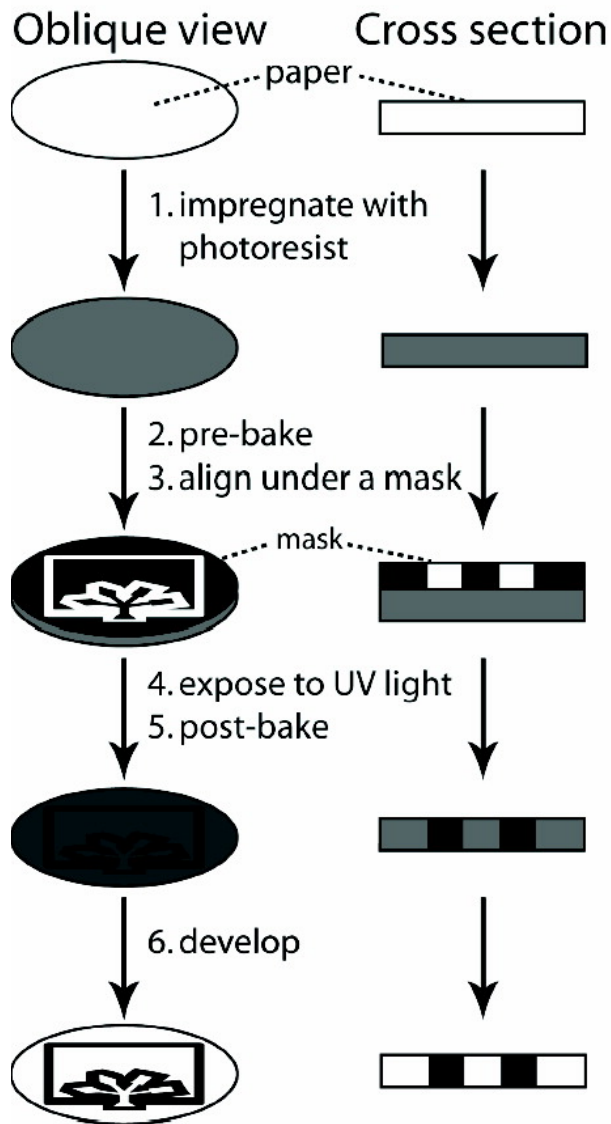


Figure 2.3. Schematic of patterning paper using photolithography

Diagram depicting the method for patterning paper into millimetre-sized channels using photolithography. Reprinted (adapted) with permission from ref.[23]. Copyright (2008) American Chemical Society.

#### 2.4.1 Wax Printing

Lu et al [24] and Carrilho et al [25] both proposed the use of wax printing for the fabrication of  $\mu$ PADs in 2009. The principle is similar to that of a generic inkjet printer whereby patterns are printed onto paper. With wax printing, the hydrophobic ink is wax and the paper, the desired

filter paper. The wax is then heated to ensure the melting of the wax through the filter paper, forming the hydrophobic barriers and hydrophilic channels.

Similar to inkjet printing, this method is advantageous as it is quick-drying and there is limited spreading of the ink after printing. It also features high-throughput with the ability to print several devices per sheet and in turn per minute [25]. Additionally, the method is simple, ideal for fast prototyping [25] and low cost- both of the instrumentation and the substrate- making it a viable option for mass production of  $\mu$ PADs.

However, the limitations include the need for thermal treatment and the poor resolution of the channels after heating in comparison to photolithography fabrication [26].

The  $\mu$ PADs produced using wax printing are compatible with aqueous systems used with biological systems including phosphate buffers, glycerol, acidic and basic solutions [25]. The wax however is incompatible with organic solvents such as methanol, ethanol and xylenes [25].

#### 2.4.2 Sol-gel

Sol-gels were initially integrated into  $\mu$ PADs to control the flow rates within their channels to mimic traditional microfluidic devices [27]. Later, in 2014, Wang et al introduced the use of sol-gel as a patterning technique to create the hydrophobic boundaries [28]. The method entails the direct inkjet printing of the sol-gel onto the paper or the selective dehydrophobisation by base etching of an MSQ impregnated paper.

Methylsilsesquioxane (MSQ) is a hydrophobic sol-gel that shows great resistance against cell lysing solutions, surfactants and other typically destructive organic solvents like glycerol, toluene and DMSO. This presents a patterning technique which has the ability to be both mass produced and quickly prototyped, as well as being more resistant than wax and AKD to aggressive chemicals.

## 2.5 Detection

Detection is imperative in the development and subsequent use of  $\mu$ PADs as the primary goal is to be able to qualify and/or quantify a desired analyte in remote or resource-deficient regions. Therefore, once the devices are made, various methods are used to impregnate or incorporate sensing into the hydrophilic areas of the designed microfluidic pattern, which is referred to as the zone. In this zone, the qualitative and/or quantitative analysis of the desired analyte is performed. In regard to the use of  $\mu$ PADs in forensic science, the sample matrix is liquid - either biological samples or solutions which contain the analyte - which easily flows to the specific sensing part of the device by capillary action which is characteristic of paper. The reagents adsorbed into the paper support, which is inert, react with the analyte resulting in some change which is then detected colorimetrically (Fig. 1.4), electrochemically, luminously or spectroscopically.

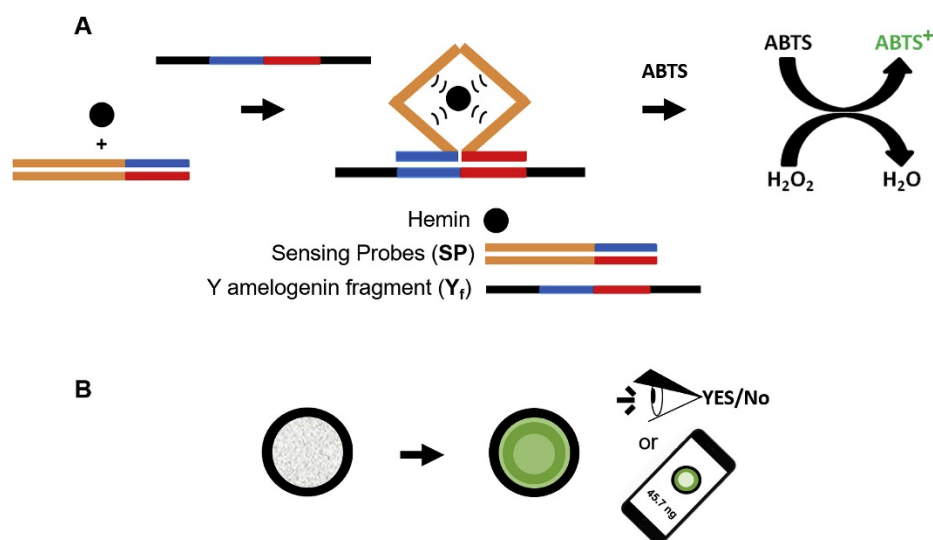


Fig. 2.4 Example of colorimetric detection.

Schematic representation of the DNAzyme formation and specific Y amelogenin fragment ( $Y_f$ ) identification of paper support. A) DNA sensing probes and hemin specifically bind to  $Y_f$  to form a 3D structure with catalytic activity able to oxidize ABTS in the presence of  $H_2O_2$ , producing green coloured  $ABTS^+$ . B) DNAzyme reaction on paper support produces an appreciable green colour in the presence of the  $Y_f$  thanks

to the oxidation of ABTS. The reaction can be monitored colorimetrically. Reprinted (adapted) with permission from ref [9] Copyright © 2020 Elsevier.

### 2.5.1 Colorimetry

The most widespread detection method is that of colorimetry and it is the detection method used throughout this thesis. Its popularity stems from its simplicity, low cost, reliability and high possibility of instrument-free detection. This detection method is based on the visual observation of a colour change or brightness resulting from a chemical or enzymatic reaction. The subjectivity that arose from the way the image was perceived by the observer and lighting conditions meant that a more reliable objective way had to be established. Imaging tools like scanners and cameras along with imaging software like Image J and Illustrator were then implemented as a reliable way to provide quantitative results. This resulted in a way to accurately correlate the amount of analyte detected to a numeric value using a colorimetric equation for example,  $\sqrt{(R - R_0)^2 + (G - G_0)^2 + (B - B_0)^2}$ . This numerical value can then be inputted into an established linear equation to give a concentration from validation studies.

### 2.5.2 Hyphenated Detection Methods

Although colorimetry is the preferred method because of its simplicity and ease of interpretation of results, sensitivity and reproducibility may be compromised with this method. Within the last decade, researchers have proposed detection methods that incorporate spectroscopy, resulting in greater sensitivities with the bonus of deciphering structural information about analytes.

Surface-enhanced Raman spectroscopy (SERS) is a powerful technique that is able to provide structural information about molecules with high detection sensitivity. This means that detection is possible at very low concentration levels of analytes. Raman spectrometers have now been miniaturized and integrated into  $\mu$ PADs providing promising avenues for on-site applications [29]. In addition, Wang et al proposed the coupling of mass spectrometers to  $\mu$ PADs for the analysis of complex samples like blood to provide chemical structures and molecular weights of analytes [30].

### 3. ESTIMATION OF TIME SINCE DEATH: ASSESSMENT OF POINT-OF-NEED DEVICES FOR DETERMINATION OF AMMONIUM CONCENTRATION IN THE VITREOUS HUMOUR

#### 3.1 Introduction

Thanatochemistry is the chemistry of death and has been established as an important facet in the determination of the time since death. More recently, scientific efforts have been geared towards finding alternative or supplementary parameters to traditional methods, to determine the post-mortem interval. These methods, which include body cooling, muscle stiffening and other body lividities, although used for centuries, present limitations in the field, due to their subjective nature. The aim, therefore, is the development of an objective and quantitative technology capable of measurable confidence intervals, precision and accuracy.

A viable biological matrix for the chemical analysis of the post-mortem interval was identified as the vitreous humour by several researchers. The vitreous humour is contained in a sac behind the eyeball and is subjected to less rapid putrefactive changes, making it ideal for post-mortem analysis [31]. Several authors have confirmed a correlation between the concentration of potassium in the vitreous humour and the post-mortem interval. However, discrepancies are evident in the data presented by the various researchers, which can be attributed both to the analytical and sampling procedures used. Tagliaro et al. highlighted the issue with the sampling procedure and recommended a micro-sampling procedure for pathologists, with a collection volume of one hundred microlitres [32]. This micro-sampling ensured that the integrity of the cell membrane was maintained, with no contamination of intracellular potassium which had resulted in skewed concentrations in the VH. Age and environmental temperature may also affect VH potassium concentrations.

In addition to the potassium ion, other components of the VH have been extensively investigated including other inorganic ions, e.g. ammonium[33], calcium [31, 34, 35], chloride [31, 34], iron (II) [36], magnesium [35] and sodium [31, 34, 35], as well as small organic molecules, such as creatinine [31, 34], glucose [31, 34, 37], lactate [34, 37], urea [34]and uric acid [34, 37]. Most of these studies have been conducted in laboratories using modern and complex technology, e.g. photometry [34], ion selective electrodes [34], enzymatic methods [34], ICP-MS [36], CE-UV [38] and LC-MSMS [39].

In 1978, van der Oever proposed the estimation of the post-mortem interval by correlating the concentration of ammonia in the vitreous humour with the time since death [40]. A gas diffusion device was used with Nessler's reagent for colorimetric detection. This report, although applied to a representative number of vitreous humour samples (150), used a method developed for a different matrix (whole blood) without a specific validation for the vitreous humour.

From this research, Gottardo et al further investigated the time-dependent linear rise of ammonium concentration in the vitreous humour[33]. The quantification of the ammonium ion in human vitreous humour (VH) samples was executed using a capillary electrophoresis method with detection at 214 nm (CE-UV). According to the authors, the increase in the ammonium concentration in the vitreous humour is the product of protein breakdown as a result of autolysis, amino acid catabolism and putrefactive phenomena.

Despite this relative abundance of analytical methods, most are based on laboratory instrumentation and require skilled personnel, hindering any possibility of analysis at the crime scene, where a preliminary PMI evaluation could be of the highest importance for the investigation [41]. The premise of this study was to therefore develop a point-of-need device that is inexpensive, reliable and user-friendly, to estimate the PMI at the death scene.

In an effort to develop such a device, Garcia et al proposed a paper-based analytical device for estimating PMI by evaluating its correlation with Fe (II) concentrations in the VH [42]. Although insightful, the proposed method refers to a negligible number of real cases (4) and specificity tests were not conducted to assess the interference of other ions and molecules present in the vitreous humour. Ultimately, there is limited literature on the correlation between the PMI and Fe (II) concentrations in the vitreous humour.

The present research was aimed at the optimisation and validation of a reliable, easy-to-use and rapid method for the determination of ammonium concentration in vitreous humour to be viable at the crime scene. This is conducted by evaluating three different analytical methods- direct mixing, a gas diffusion device and  $\mu$ PAD. The method was based on the selective interaction between Nessler's reagent and molecular ammonia, which is directly related to the time since the death.

## 3.2 Materials and Methods

### 3.2.1 Chemicals

All chemicals were of analytical reagent grade. Ammonium chloride, calcium chloride, magnesium chloride, Nessler's reagent, potassium chloride, sodium chloride and sodium hydroxide were all obtained from Sigma-Aldrich (Darmstadt, Germany). Creatinine, lactic acid, and urea were purchased from Carlo Erba Reagent (Milan, Italy). A model Purelab1-Chorus 3 water purification system (Elga Veolia, High Wycombe, United Kingdom) was utilized to obtain ultra-pure water for preparation of all the solutions. Hydrophobic polytetrafluoroethylene (PTFE) membrane with a 0.45mm pore with a diameter of 47 mm was purchased from Merck Millipore (Darmstadt, Germany).

### 3.2.2 Sample collection

Vitreous humour samples were collected from 27 forensic deaths, including road accidents, drug overdoses and firearm homicides. The PMIs, which were precisely known, ranged between 6 to 163h and the victims were between 21 to 75 years old. The samples were collected from both eyes by needle puncture and gently suctioned from the vitreous humour sac with a plastic syringe (insulin type). The samples were anonymised and stored at -20 °C until analysis.

### 3.2.3 Direct Mixing

One hundred microliters of Nessler's reagent were mixed with 100µL of sample in an Eppendorf tube, and the image recorded using a smartphone (iPhone 6).

### 3.2.4 Gas diffusion device

The method was based on a colorimetric reaction between molecular ammonia and Nessler's Reagent. Two hundred microliters of sample were added in a micro test tube (PCR sample tube) with 30 mg of NaOH, the device was then covered with a polytetrafluoroethylene (PTFE) filter and 30µL of a diluted Nessler's reagent was dropped on the filter.

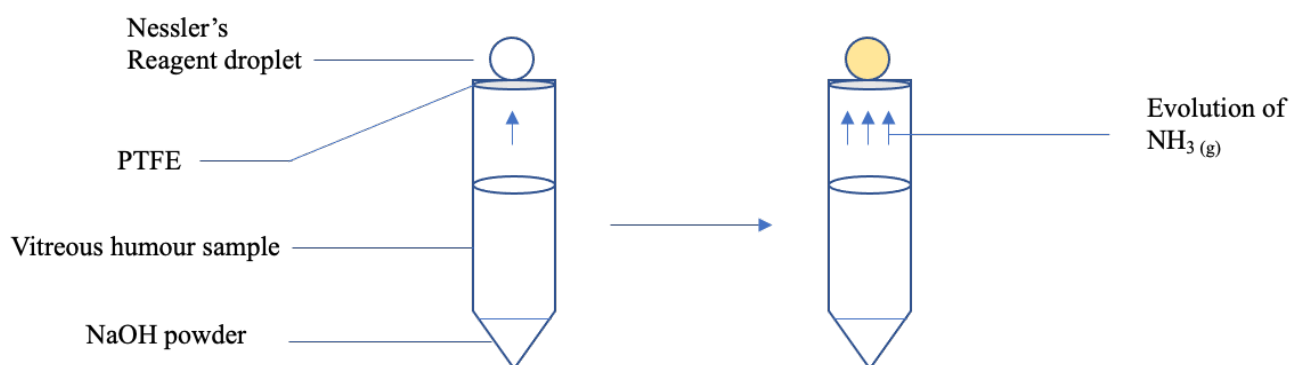


Fig. 3.1 Schematic of gas diffusion device.

The diagram shows the pulverised NaOH at the bottom of the PCR tube, then after the addition of the vitreous humour sample, the device is covered with PTFE. Overtime, as ammonia gas is evolved, the Nessler's reagent droplet turns from colourless to yellow.

### 3.2.5 Fabrication of $\mu$ PAD

The design was created using Apple Pages and printed using a wax printer on Whatman filter paper (GE Healthcare, Life Sciences, Whatman Grade 1 CHR). The design comprised 5mm-diameter circles arranged in a 5x4 rectangle, on either side of the device that perfectly overlap when the device is folded. After wax printing, it was then placed in an aluminium foil holder, which was placed on a hot plate at 150 °C for 2 ½ minutes. The device was folded to acquire the resultant microfluidic device, comprising two faces, fastened together with staples.

Five microliters of 10 M NaOH were spotted on one of the internal sides and five microlitres of Nessler's reagent spotted on the opposite side. The spots were allowed to dry and stapled together for subsequent analysis of the VH samples. Thirty microliters of the vitreous humour sample were spotted on Face 1 and the device was turned to reveal Face 2 after 30- 60 seconds depending on the viscosity of the VH sample.

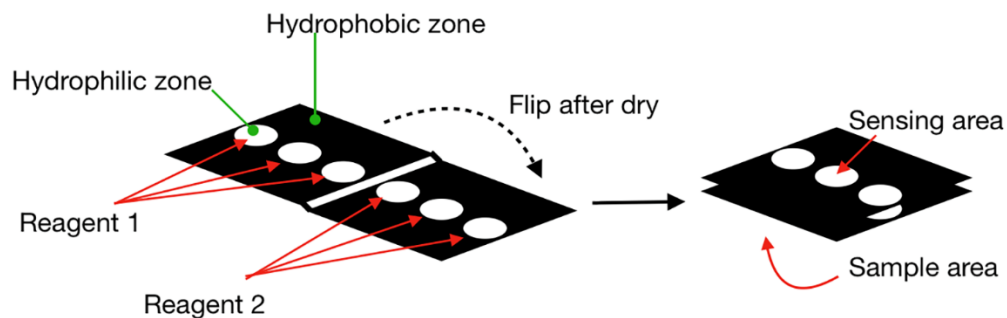


Fig. 3.2 Schematic of  $\mu$ PAD used in the determination of ammonium concentrations in vitreous humour samples. [8]

### Analysis of samples

A smartphone camera (iPhone 6, Apple Inc., Cupertino, CA, US) was used to record the image of the sensing part of each device. All photos were taken with the camera flash, the phone in a marked position and the device positioned in a Styrofoam box to maintain the consistency of the lighting. The evaluation of the interaction between ammonia and Nessler's reagent was estimated by a deconvolution of the red, green and blue components using the ImageJ 1.53a software to obtain the RGB distance ( $\Delta$ RGB) by the following equation:

$$\sqrt{(R - R_0)^2 + (G - G_0)^2 + (B - B_0)^2}$$

In the above equation, the values  $R_0$ ,  $G_0$  and  $B_0$  correspond to the components R, G and B of a saline solution, which was analysed for each test and considered as reference value. While the value R, G and B are the red, green and blue components of the sample area.

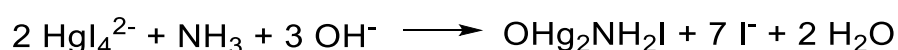
### 3.2.6 Validation

The validation parameters investigated were linearity, limit of detection (LOD), upper limit of quantification (ULOQ), lower limit of quantification (LLOQ), specificity and within-run and between days precision and accuracy. The specificity of each experiment was investigated in the presence of the potential interferences from other biological components of the VH. Saline solutions (0.9% NaCl) spiked with calcium, chloride, creatinine, lactate, potassium, sodium and urea were analysed individually to assess their effects on the colorimetric response. The linearity was evaluated within a range of ammonium concentrations from 0.5 to 5.0 M, and

consequently the calibration curve was chosen between the limits of the best linearity. The limit of detection (LOD) was defined as the lowest concentration at which a colorimetric response was visually evident to three different operators. The lowest limit of quantification (LLOQ) was the lowest concentration of ammonium at which the RGB value recorded showed an accuracy and precision in the range of 25% (from three replicates for six runs). Conversely, the upper limit of quantification (ULOQ) was the highest concentration of ammonium at which the recorder RGB values met the same criteria. Reproducibility and accuracy of the method were tested by analysing ammonium solutions at the LLOQ and ULOQ and three intermediate concentration levels. These parameters were assessed by the analysis of three replicates for each concentration for six different days. Within-run and between days precision were determined by the calculation of %RSD of the corresponding average RGB values. The validation criteria required that %RSD values were less than 20%, whereas at LLOQ and ULOQ they were required to be less than 25%. Accuracy was expressed as the percentage of the theoretical concentration (acquired from the calibration curve) experimentally measured in fortified samples with known concentrations of ammonium. The accuracy value required was in the range 85-115%.

### 3.3 Results and Discussion

Nessler's reagent selectively reacts with ammonia, in a basic environment, a reaction explained by Sarkar and Gosh in 1955. The reaction is denoted as follows:



A challenge for forensic scientists and pathologists was the creation of a portable, point of need test that was able to determine the post-mortem interval (PMI) of a corpse. Over four decades ago, a gas diffusion device, which presented a solution, was developed by van den Oever [40]. This device was able to estimate the PMI by evaluating the evolution of ammonia spectrophotometrically (absorption wavelength 420 nm) and was tested on 150 VH samples. A strong correlation between the concentration of ammonium and the post-mortem interval was reported with a linear ammonium VH increase for the first 100 h post-mortem after sudden deaths.

The device, however, does not satisfy the ASSURED guidelines highlighted earlier and so, did not have great applicability in the field. Firstly, the procedure involves the use of equipment- a rotator to aid in the diffusion of ammonia gas, as well as a UV spectrophotometer for detection. Another challenge of the method included its manual complexity, which includes the use of other laboratory utensils, which results in difficulty with standardisation. Due to its apparent lack of practicality, research into point-of-need devices for the determination of the PMI had ceased.

The first objective of this research is thus the development of a modified gas diffusion device with a specific validation for vitreous humour, an instrument-free, simpler method and detection, as well as the determination of PMIs greater than 100h.

Additionally, as the overall aim of this study is to propose a method that can be used at the point-of-need, for the estimation of time of death, the development of a novel paper-based microfluidic device was explored. The use of paper-based microfluidic devices as point-of-need tests (PONTs) for various areas of applied analytical chemistry, which replace traditional instrumentation, has been extensively researched in recent years, and so was determined to be a feasible solution.

In regard to instrument-free quantification and detection methods, the use of a smartphone was investigated, a device widely owned, for detection. For quantification, the approach used was based on the deconvolution of the colour components of the image and the correlation of one, or more components, with the concentration of the analyte.

On these grounds, the second objective of this research was aimed at the development of a novel microfluidic paper-based device for the analysis of ammonium in VH intended for potential use at the crime scene in combination with a smartphone as the detection and data processing device.

The research included four different parts: a) optimisation studies for gas diffusion device; b) preliminary assessment of the suitability of the Nessler's reagent for the analysis of VH (direct mixing study); c) design and validation of the microfluidic paper-based device and gas diffusion device and d) analysis of real samples.

### 3.3.1 Optimisation studies for gas diffusion device

In order to obtain the optimal conditions for the analysis, the following parameters were investigated: concentration of Nessler's reagent, the volume of the reagent, length of time for colour development and sample volume. The most suitable parameter was determined by the best RGB distance obtained from the optimisation study.

The optimal concentration of Nessler's reagent compatible for the analysis was investigated by testing 4 different dilution ratios 1:1, 1:2, 1:3 and 1:8 at 4 different ammonium concentrations (0.5, 1.0, 1.5 and 2.0mM) overtime. The most suitable reagent concentration was determined as 1:3, because it showed the most distinction (with no overlap) in RGB values from concentration to concentration, as was evident with other Nessler's reagent dilutions. This dilution of Nessler's reagent was used for the rest of the optimisation studies.

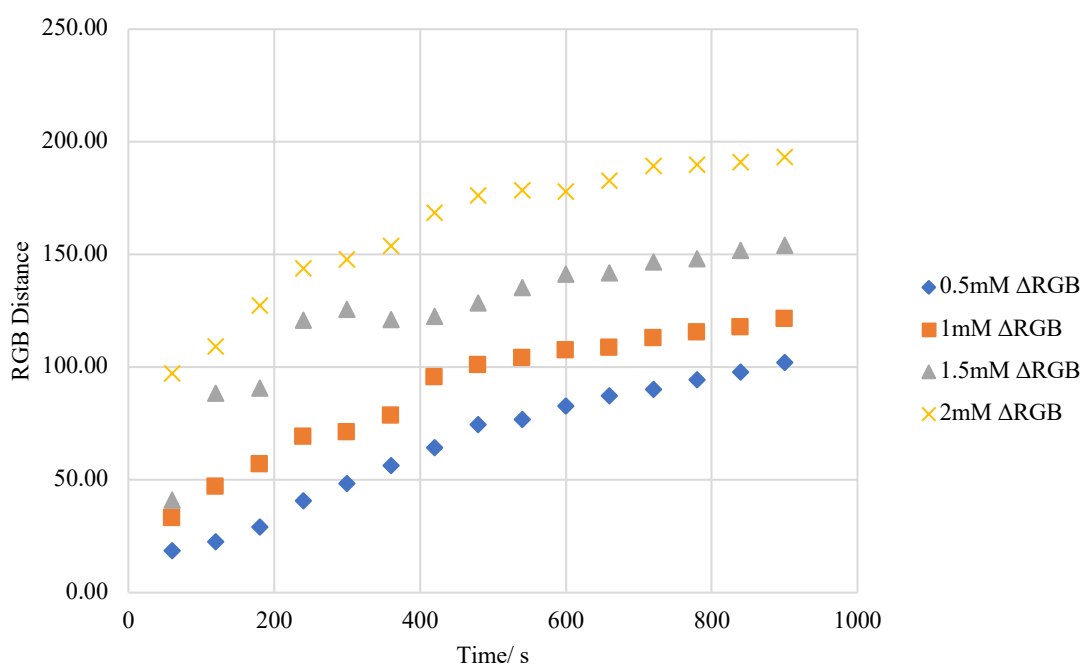


Fig. 3.3 Evaluation of best dilution of Nessler's reagent.

1:3 is the only dilution ratio that showed distinction between ammonium concentrations.

The volume of the reagent required was then determined as 30  $\mu\text{L}$  after volumes of 5, 30, 50 and 100  $\mu\text{L}$  were tested and showed no critical distinction above 5  $\mu\text{L}$ , among them. This discovery is favourable as it allows for the use of disposable plastic pipettes, which can be used at the crime scene.

Subsequently, the length of time for colour development was examined by monitoring at 60 s intervals between 0 and 900s at 0.5 and 2.0 mM of ammonium. A constant gradient of RGB distance was obtained from 180 s and so, images were taken for analysis at this point.

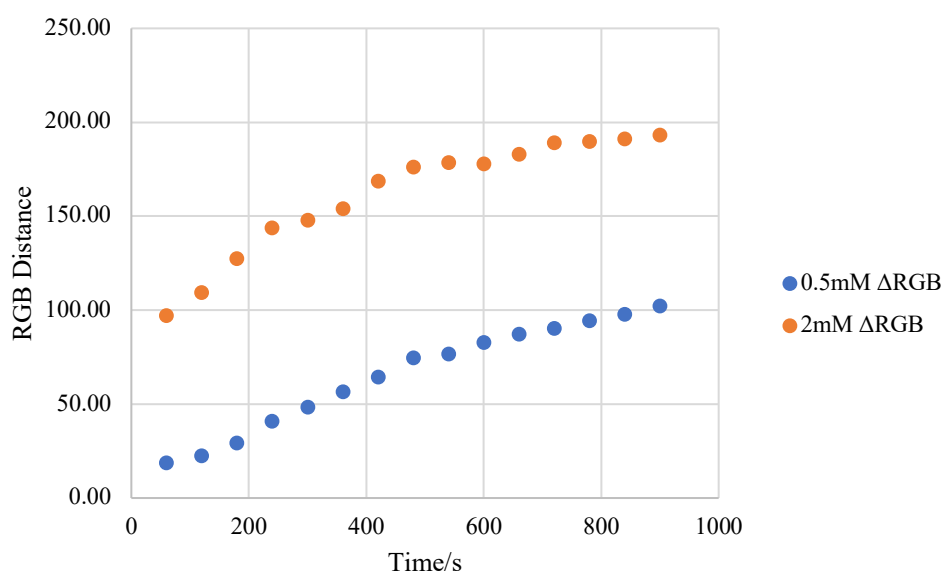


Fig. 3.4. The estimation of the best time interval to record image.

Based on the change in colour, expressed as the RGB distance, from 0 to 900 s. The study was conducted at two ammonium concentration levels- 0.50 mM (blue) and 2.00mM (orange).

Finally, the principle of this gas diffusion device is the formation of a “headspace”, which the evolved ammonia gas populates, and then diffuses across a membrane (PTFE), thereafter interacting with the Nessler’s reagent, giving a colorimetric response. The area of this headspace and volume of ammonia evolved are therefore important in the outcome of this method. Three sample volumes were evaluated- 50, 200 and 400  $\mu\text{L}$ , with 200  $\mu\text{L}$  chosen as the optimal sample volume. Although a direct correlation between sample volume and RGB distance was observed, based on the requirement for micro sampling techniques highlighted before, 200  $\mu\text{L}$  was regarded as the best compromise.

It is also worth noting that approximately 30 mg of NaOH powder was used, as determined by a scoop of the micro spatula. In any case, NaOH is in excess in this reaction as ammonium is the limiting reagent.

*Table 3.1: Summary of parameters investigated to achieve the optimal analysis conditions for gas diffusion device.*

PARAMETER	RANGE INVESTIGATED	OPTIMAL CONDITION DETERMINED
Nessler's reagent concentration	1, 1:1, 1:3, 1:4, 1:8	1:3
Volume of reagent	5, 30, 50, 100 $\mu\text{L}$	30 $\mu\text{L}$
Time for colour development	0- 900 s	180 s
Sample volume	50, 200, 400 $\mu\text{L}$	200 $\mu\text{L}$

### 3.3.2 Preliminary assessment of the suitability of the Nessler's reagent for the analysis of VH (Direct mixing study)

In order to develop a viable microfluidic paper-based device, a proof-of-concept study was conducted whereby the colorimetric reagent was tested in solution by adding the reagent directly to VH samples.

The same optimisation methods as described previously, were carried out on this direct mixing method. The concentration of Nessler's reagent, the volume of reagent, length of time for colour development and sample volume were all evaluated. For simplicity, a summary of the optimisation studies is highlighted in Table 2.

Table 3.2: Summary of parameters investigated to achieve the optimal analysis conditions for direct mixing analysis.

PARAMETER	RANGE INVESTIGATED	OPTIMAL CONDITION DETERMINED
Nessler's reagent concentration	1, 1:1, 1:3, 1:4, 1:8	1
Volume of reagent	5, 30, 50, 100 $\mu\text{L}$	100 $\mu\text{L}$
Time for colour development	0- 600 s	10 s (colour evolved very quickly)
Sample volume	50, 100, 200, 400 $\mu\text{L}$	100 $\mu\text{L}$

The sensitivity of the procedure was established by the addition of Nessler's reagent to saline solutions with decreasing concentrations of ammonium. The colour change of the solution, after a reaction time of 10 s, was observed by the naked eye and measured using the smartphone camera. The lowest detectable concentration was 0.30 mM, showing a sensitivity which meets the ammonium concentrations usually found in real samples. A range of 0.30 – 1.50 mM was achieved using this method. However, the chromogen,  $\text{OHg}_2\text{NH}_2\text{I}$ , precipitates out of solution, resulting in a solution colour that is transitory and so, not practical for on-site usage. In addition, solutions containing the main components of the vitreous humour, as reported in a study based on over 230 autopsies (i.e., sodium, potassium, chloride, calcium, urea, creatinine and lactate), were tested with the reagent to establish analytical selectivity (Fig. 3.5).

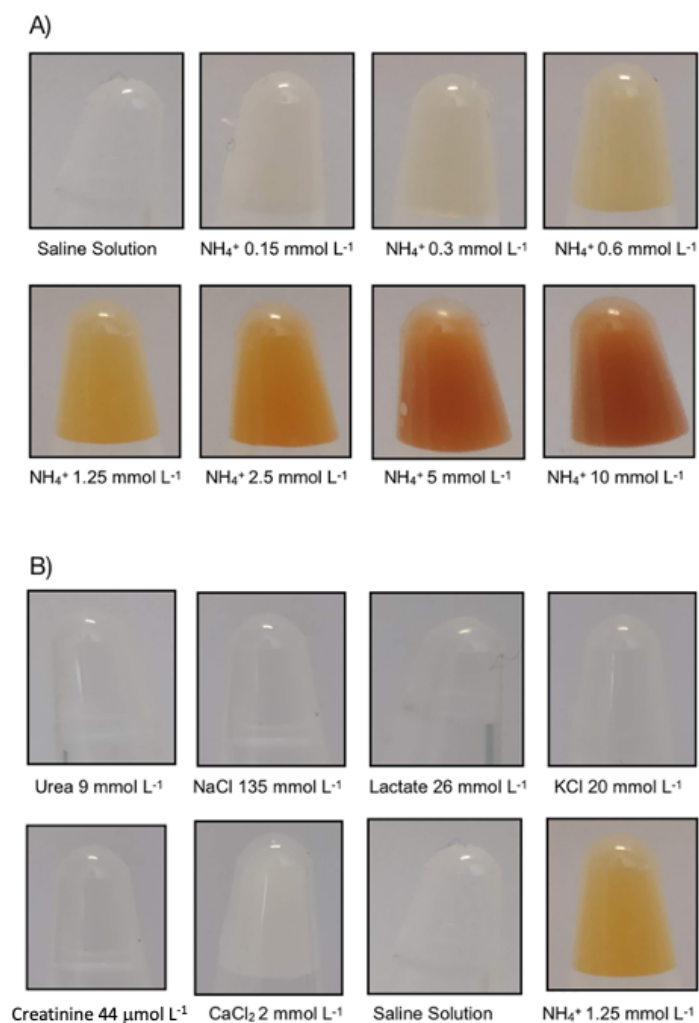


Fig. 3.5 Linearity and specificity studies for direct mixing method

A) Direct mixing of varying concentrations of ammonium solutions with Nessler's reagent; B) Specificity studies to determine the interaction between Nessler's reagent and other ions which are usually present in the VH matrix [8].

### 3.3.3. Design and validation of the microfluidic paper-based device and gas diffusion device

Based on the satisfactory results of the feasibility study, efforts were directed towards the conversion of the direct mixing method into a paper-based device to circumvent the issue of the formation of the chromogen precipitate. The design of the device was devised to ensure compatibility with use on-site, such as at a crime scene. As demonstrated in the feasibility study, the selectivity of the reagent permits the use of sample without treatment. Consequently, the analysis can be carried out by an operator by simply depositing a drop of the VH fluid

directly onto the paper support. After the addition of the sample to the hydrophilic circle, in few seconds an evident colour change on the opposite side was observed (Fig. 3.1). In an optimization process, the influence of temperature on the colour development was studied at 4 °C, 20 °C and 35 °C. As shown in Fig. 3.6, no substantial effect on the RGB distance was observed in the temperature range investigated at two ammonium concentrations (0.75 and 1.25 mM).

The stability of the reagent absorbed on the paper was tested. The device, with the dried reagents, maintained reactivity for at least ten days at two concentration levels of ammonium-0.75 and 1.25 mM, when refrigerated at 4 °C. While the stability was maintained for one day if stored at room temperature by keeping it away from light sources. The oxidative action of the atmosphere at room temperature results in the decomposition of the active ion in Nessler's reagent is the proposed reason for this instability.

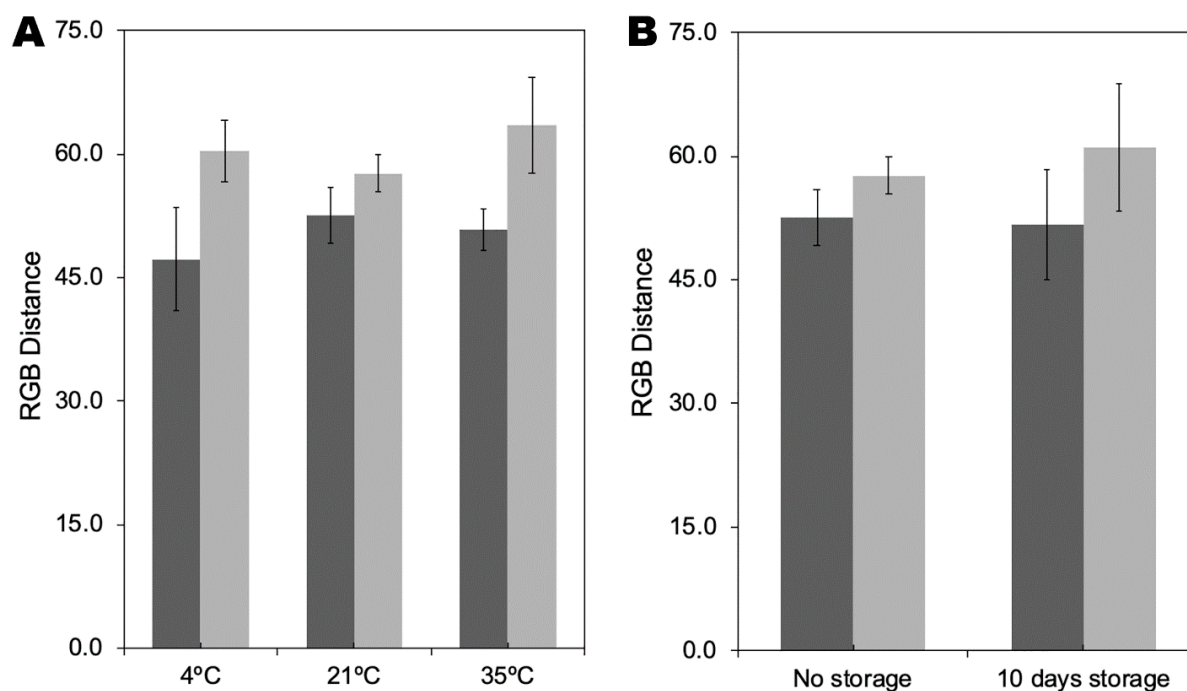


Fig 3.6 Effect of temperature and storage on RGB distance

A) Depiction of variance of RGB distance, with standard deviation error bars, based on the sample temperature 4, 21 and 35 °C at two concentration levels (0.75 and 1.25 mM).  
 B) Depiction of variance of RGB distance to assess the reactivity of the device stored in a refrigerator at 4 °C for ten days [8].

### 3.3.4 Method validation

The method validation was then performed according to the usual parameters stated in the guidelines of forensic analysis for each method, taking into consideration the semi-quantitative nature of the test. In short, validation included the assessment of specificity, limit of detection (LOD), lower limit of quantification (LLOQ), calibration curve, within-run and within-day precision and accuracy. The selectivity of the methods was evaluated according to the same procedure as that used in the proof-of-concept. Also, the testing of both paper-based microfluidic device and gas diffusion device was successful since no colour interferences were observed.

The LOD was determined as the lowest concentration, which could be discriminated from the saline solution by naked-eye observation on each one of three replicates and by using the smartphone recording. The LOD for the GD device and  $\mu$ PAD analyses was 0.3125 and 0.4mM, respectively. The LLOQ was identified as the lowest concentration which could be determined with accuracy and precision, within 75-125% and  $\leq 25\%$ , respectively, and was identified as 0.3125mM for GD and 0.5 mM for  $\mu$ PAD. The linearity of the methods was confirmed in the range of concentration between 0.3125 and 1.5mM for GD and 0.50 and 1.5 mM for  $\mu$ PAD. The %RSD of within-run and between days precision, evaluated at five concentration levels including LLOQ and ULOQ, and three intermediate points of the calibration curve- (0.3125, 0.5,0.75,1.0 and 1.5 mM) for GD and (0.50, 1.50, 0.75, 1.00 and 1.50 mM) for  $\mu$ PAD. The %RSDs were  $\leq 15.7$  for GD and  $\leq 13.2\%$  for  $\mu$ PAD. In these analyses, analytical inaccuracy ranged from 85.9% to 114.0% for GD and 85.9% to 111.9% for  $\mu$ PAD, of the target concentrations. Within-run and between days precision as well as accuracy were adequate with at least 75% of calibrator levels showing differences in the nominal concentration within  $\pm 25\%$  for the lowest (LLOQ) and the highest (ULOQ) calibrator level, while it was within  $\pm 20\%$  for the other calibrator levels for both methods.

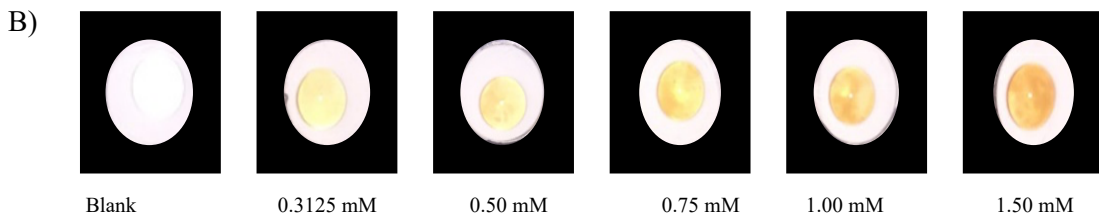
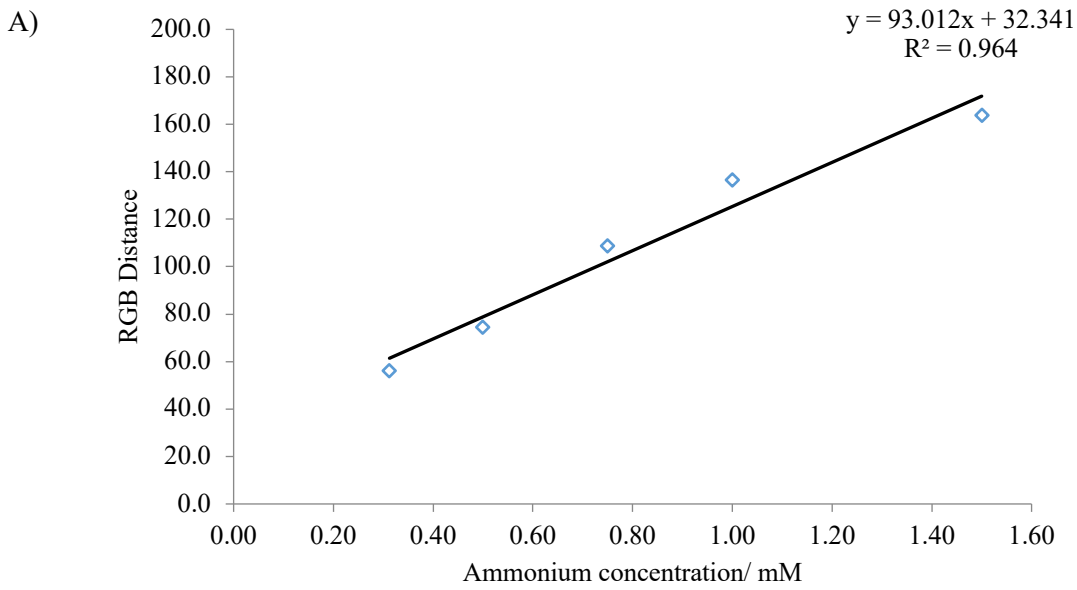
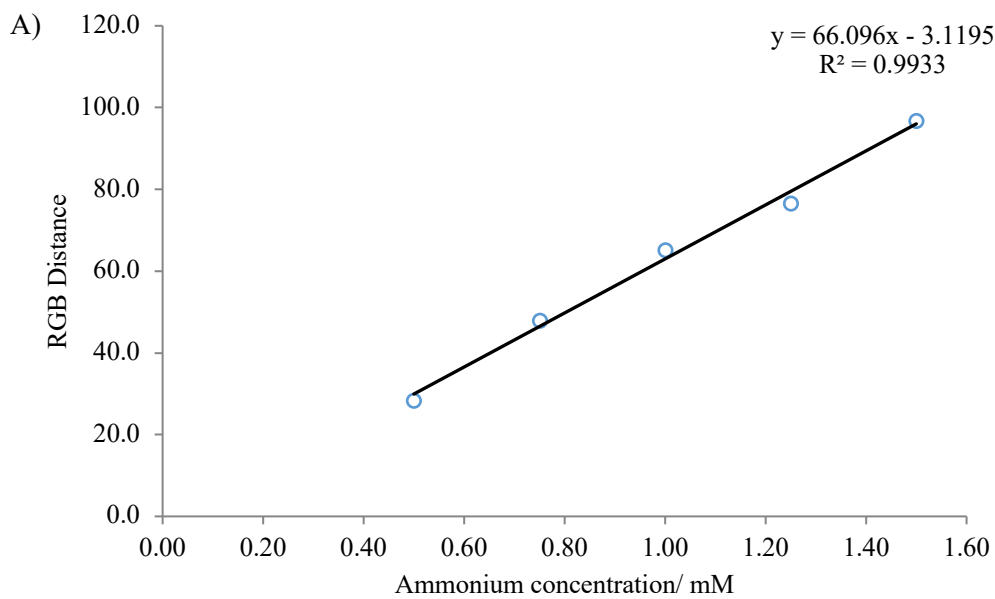


Fig. 3.7 Linearity and corresponding images of GD method

A) Linearity of gas diffusion method B) Optical images showing the linearity of the GD method.



B)

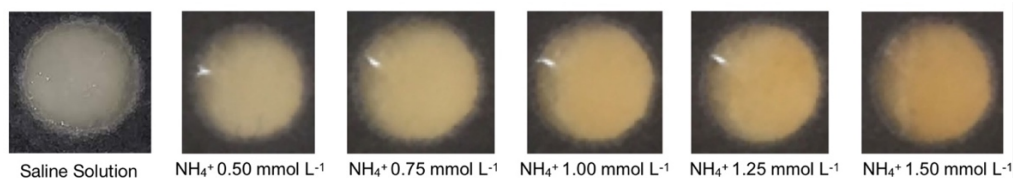


Fig. 3.8 Linearity and corresponding images of  $\mu$ PAD method

A) Linearity of  $\mu$ PAD method (0.5-1.5 mM) B) Optical images showing the linearity.

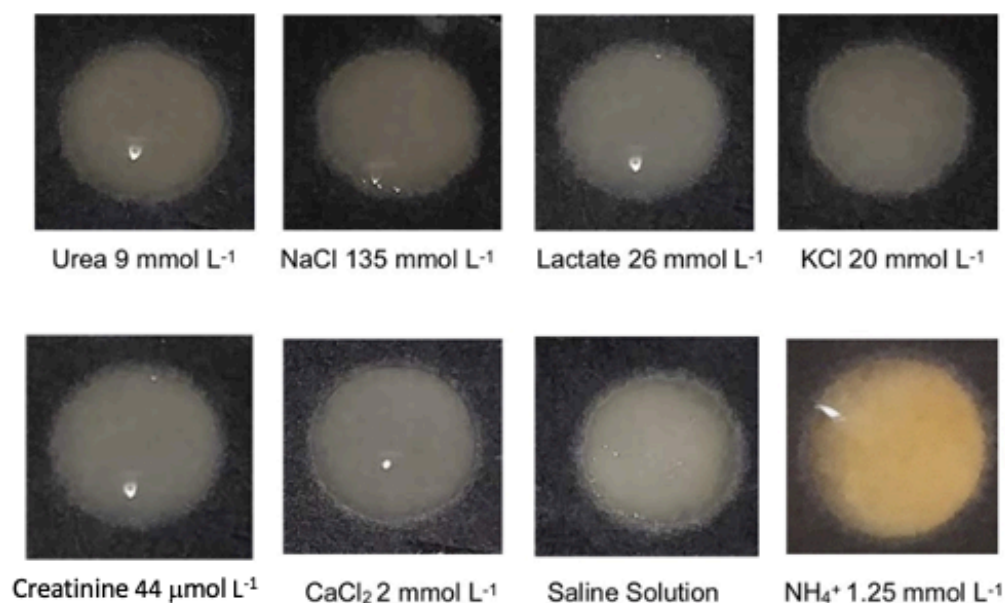


Fig. 3.9 Specificity studies for  $\mu$ PAD method [8].

### 3.3.5 Analysis of real samples

#### 3.3.5.1 Comparison of proposed methods with capillary electrophoresis- ultraviolet spectroscopy (CE-UV) method

The validity of each method was then explored by testing vitreous humour samples from forensic deaths. A total of 27 VH samples were tested, using each method, with a known ammonium concentration range, established using a method based on capillary electrophoresis, of 0.2 to 3.76 mM [6]. The analysis of the data showed that the  $\mu$ PAD method was applicable

between the range of 0.2 to 1.5 (22 VH samples), whereas the GD method was valid against the full range tested (27 VH samples).

The use of the  $\mu$ PAD and gas diffusion devices showed the best correlation with the corresponding equations as follow:

- (i)  $\mu$ PAD:  $y = 0.9271x$  [ $R^2 = 0.9675$ ]
- (ii) GD:  $y = 1.0725x$  [ $R^2 = 0.9226$ ]

The results for the direct mixing method were not promising with a regression of 0.3.

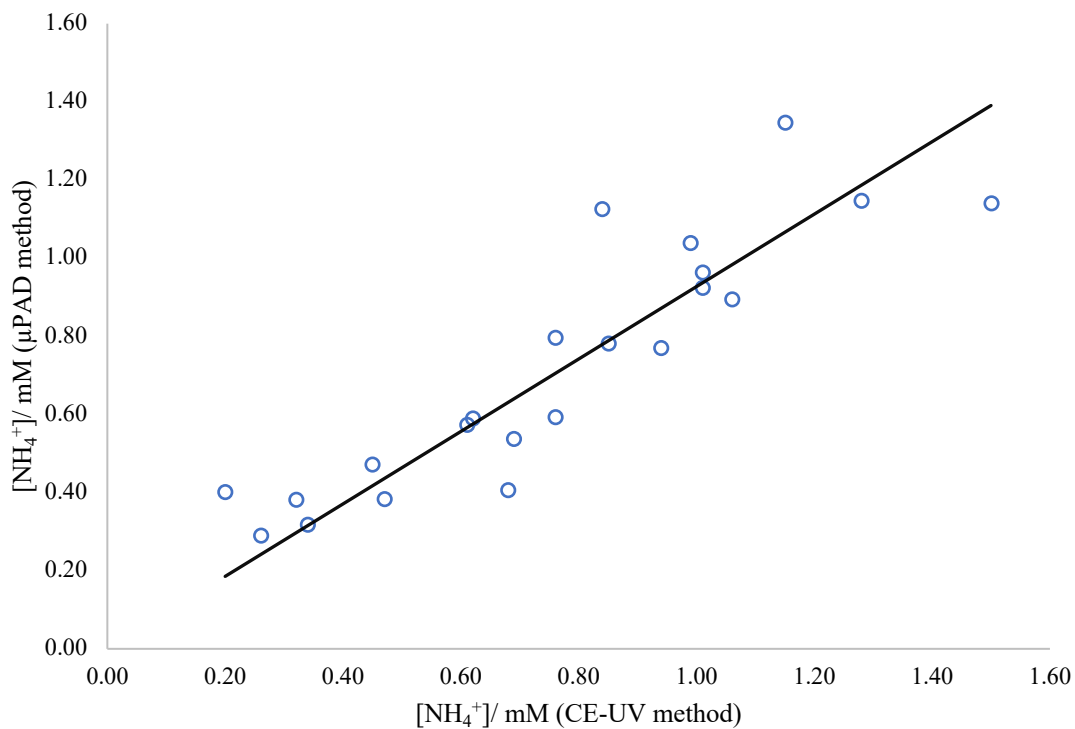


Fig 3.10: Correlation between CE-UV and  $\mu$ PAD method

The correlation between the ammonium concentration of 22 VH samples using the established CE-UV method (x-axis) and the  $\mu$ PAD method (y-axis);  $R^2 = 0.9675$ .

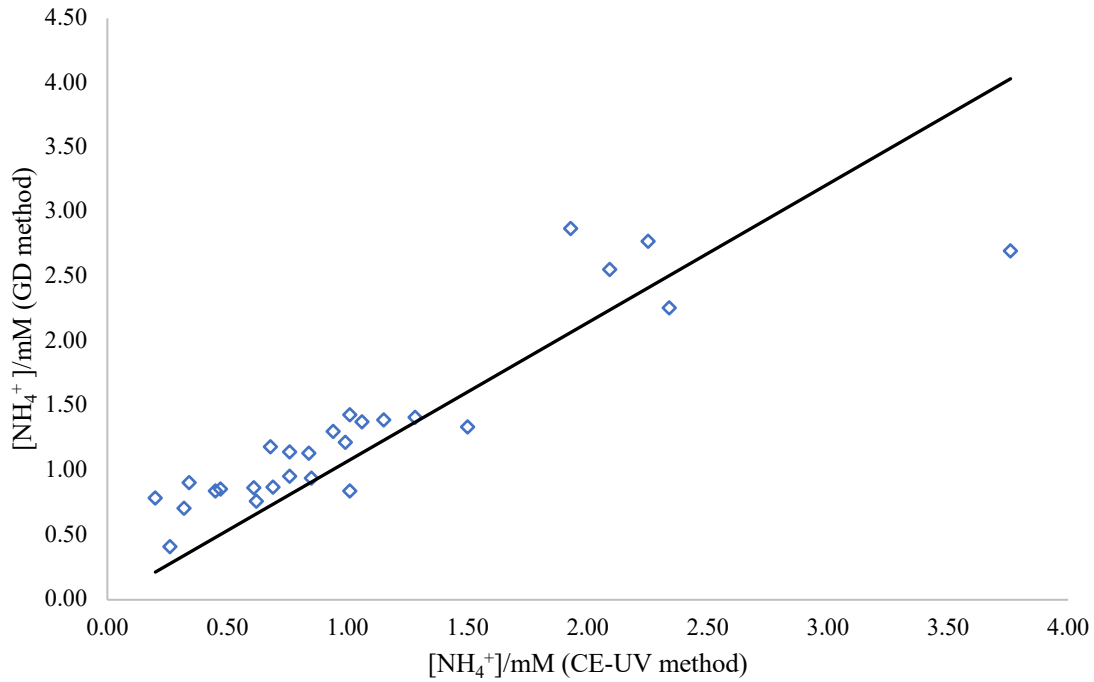


Fig 3.11: Correlation between CE-UV and GD method

The correlation between the ammonium concentration of 27 VH samples using the established CE-UV method (x-axis) and the GD method (y-axis);  $R^2 = 0.9226$ .

### 3.3.5.2 Comparison of proposed methods with established PMIs

The two methods that showed pertinence-  $\mu$ PAD and GD- were then used to evaluate the relationship between the ammonium concentration and the post-mortem interval (PMI). The  $\mu$ PAD method was used to test PMIs of 6 to 106 h (22 VH samples), and the GD method was used to test PMIs up to 163 h.

The relationship between the PMI values and the ammonium concentration for each method is denoted below:

iii)  $\mu$ PAD:  $y = 0.0138x$  [ $R^2 = 0.9587$ ]

iv) GD:  $y = 0.0179x$  [ $R^2 = 0.9252$ ]

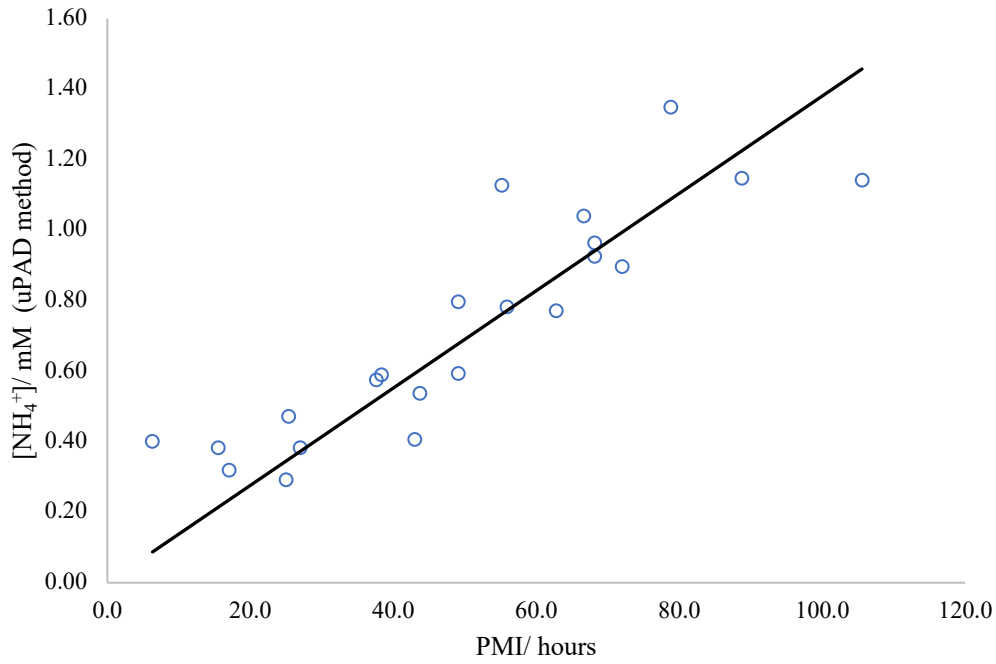


Fig 3.12: Correlation between PMI and  $[\text{NH}_4^+]$  from  $\mu\text{PAD}$  method

The correlation between known PMI values (x-axis) of 22 VH samples and the ammonium concentrations from  $\mu\text{PAD}$  method (y-axis);  $R^2 = 0.9587$ .

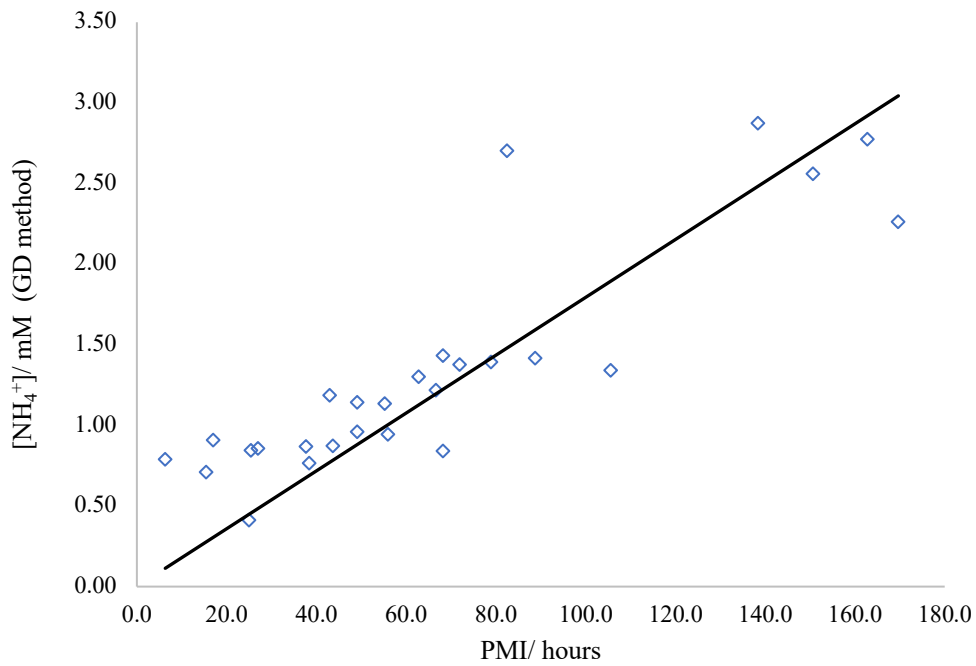


Fig 3.13: Correlation between PMI and  $[\text{NH}_4^+]$  from GD method

The correlation between known PMI values (x-axis) of 27 VH samples and the ammonium concentrations from GD method (y-axis);  $R^2 = 0.9252$ .

Finally, a provisional application of each method for the estimation of PMI was carried out on the respective sample sets, after having removed each case from the reference curve. Under these conditions, the average error of PMI estimation was 14.2 hours for the GD method and 13.1 hours for the  $\mu$ PAD method.

### 3.3.6 Overall comparison of three investigated methods

Based on the criteria outlined by the WHO for point-of-need devices, the compliance of each method tested is summarised in Table 1. Notably, although the direct mixing method showed great linearity with standard ammonium solutions, as well as great specificity against other ions and molecules present in the VH matrix, this was not transferrable when used on real VH samples. This method is therefore not compliant with the sensitivity and specificity denoted by the ASSURED criteria. The main distinction between the two methods which showed viability-  $\mu$ PAD and GD- is that the paper-based microfluidic device showed both user-friendliness and deliverability to end users.

*Table 3.3: Comparison of each method with ASSURED criteria*

	$\mu$ PAD	GD	DM
Affordable	Yes	Yes	Yes
Sensitive	Yes	Yes	No
Specific	Yes	Yes	No
User friendly	Yes	No	Yes
Rapid and robust	Yes	Yes	Yes
Equipment free	Yes	Yes	Yes
Deliverable to end users	Yes	No	Yes

### 3.4 Conclusion

After investigating three different equipment-free methods for estimating the time since death, the use of a paper-based microfluidic device has shown the most promise and fulfils the ASSURED criteria. The method is simple, rapid, portable, does not require skilled personnel and provides results within a few minutes. It has highlighted the possibility offered by a low-cost microfluidic paper-based device and a simple detection and data treatment procedure to accurately measure ammonium in the VH, as a simple tool for inferring the PMI without the use of laboratory instrumentation. In particular, the measurement of the RGB distance, a parameter easily measurable using common free apps for smartphones, has proven to be a reliable parameter for the quantification of Nessler's reaction chromogen. This RGB distance is related to the ammonium concentration in the VH, which in turn is related to the PMI. It is therefore very promising for field applications, at the crime scene, in addition to the traditional methods of forensic pathology which are well known in this field, such as temperature, lividities and dehydration.

### 3.5 Future research

Future research should concentrate on the acquisition of more vitreous samples with a wider range of PMIs.

## 4. THE DEVELOPMENT OF A PAPER-BASED MICROFLUIDIC DEVICE AS A PRELIMINARY SCREENING TEST FOR DRUGS OF ABUSE IN URINE: DETERMINATION OF CONCENTRATION OF URINARY CREATININE

### 4.1 Introduction

Creatinine is a very important molecule in forensic toxicology. The detection and quantification of creatinine is the preliminary step in the quantification of drugs of abuse. Its concentration in the urine determines the viability of the sample and so, indicates whether the sample can undergo further analysis or not.

Urine is a viable biofluid because it can be used to detect and quantify alcohol, amphetamines, barbiturates, benzodiazepines, cocaine, marijuana, methamphetamine, opioids and phencyclidine (PCP) as well as some of their metabolites. In general, alcohol and drugs vary significantly in their window of detection, with the greatest contributor being the fat solubility of the molecule, and other factors that also depend on the substance, the amount and frequency of the substance taken. According to Hadland et al [43], there is a window of detection in urine of one day to several weeks. There are several advantages of using urine as the biological matrix for drug detection including its availability in sufficient quantities, non-invasive specimen collection, higher concentrations of parent drugs and metabolites when compared to blood, availability of point-of-need tests (PONTs) and well researched testing techniques.

As previously mentioned, the quantification and detection of creatinine is the preliminary step in any drug analysis. In routine analysis, immunoassay is the most widely used in the quantification of creatinine due to its inherent specificity, high-throughput, high sensitivity and no sample preparation [44]. Other methods employed include enzymatic method [45], flow injection analysis [46], HPLC [47-52], capillary electrophoresis [53-56], GC-MS and LC-MS-MS [57-60].

The most widely employed colorimetric method for the determination of creatinine is the Jaffé's method, which was proposed by Max Jaffé in 1886 [61]. The method was then adapted for clinical applications by Otto Folin in 1919 [62]. Picric acid (PA) reacts with creatinine in an alkaline solution to yield a coloured complex.

Despite the extensive use of the Jaffé's method in the clinical field, it is highly non-specific. Compounds including glucose, pyruvate, ascorbate, and bilirubin are present in urine and also interact with picric acid in an alkaline solution [63]. In 1936, three independent research groups- Langley and Evans [64], Bollinger [65] and Behre [66]- all proposed a procedure for the determination of creatinine using 3,5-dinitrobenzoic acid (DNBA) in an alkaline solution. This method introduced a kinetic variant of the Jaffé's method in order to increase specificity and results in the formation a creatinine-dinitrobenzoate coloured complex.

Nessler's Reagent (NR) has been extensively studied in literature and is used for the selective detection and quantification of ammonia [67, 68]. In studies previously carried out by our group, it was found that the reagent interacted with creatinine in a way distinct to that of ammonia. The structure of creatinine contains two amine groups and would explain the colorimetric response of the reagent albeit with a different hue from that of ammonia.

The last decade has seen a significant emergence in the study and use of microfluidic paper-based analytical devices ( $\mu$ PADs) for colorimetric chemical sensors. In 2007, Martinez et al [15] proposed the first procedure for the development of  $\mu$ PADs with several methods subsequently developed [69]. Sununta et al [70] developed a method to determine the concentration of urinary creatinine using  $\mu$ PADs. Although innovative, the paper lacks a substantial number of real cases (5), only uses the Jaffé's method, which as previously stated, has its limitations. The intended purpose of the device also differs from this study, and so, linearities, validation studies and data set ranges are different to that presented in this paper.

The present study evaluates the use of paper-based microfluidic devices to determine the concentration of urinary creatinine employing three different colorimetric reagents- picric acid, 3,5-dinitrobenzoic acid and Nessler's reagent.

## 4.2 Materials and Methods

### 4.2.1 Chemicals

Nessler's Reagent, Picric acid, sodium hydroxide, 3,5-dinitrobenzoic acid (DNBA), urea, trisodium citrate dihydrate, sodium chloride, ammonium chloride, calcium chloride, sodium oxalate, disodium hydrogen phosphate and MilliQ water. All the reagents were analytical reagent grade and acquired from Sigma-Aldrich (Darmstadt, Germany).

### 4.2.2 Fabrication of $\mu$ PAD

The design was created using Apple Pages and printed on Whatman filter paper (GE Healthcare, Life Sciences, Whatman Grade 1 CHR) then placed in an aluminium foil holder, which was placed on a hot plate at 150 C for 2 ½ minutes. The device was folded to acquire the resultant microfluidic device, comprising three faces fastened together with staples.

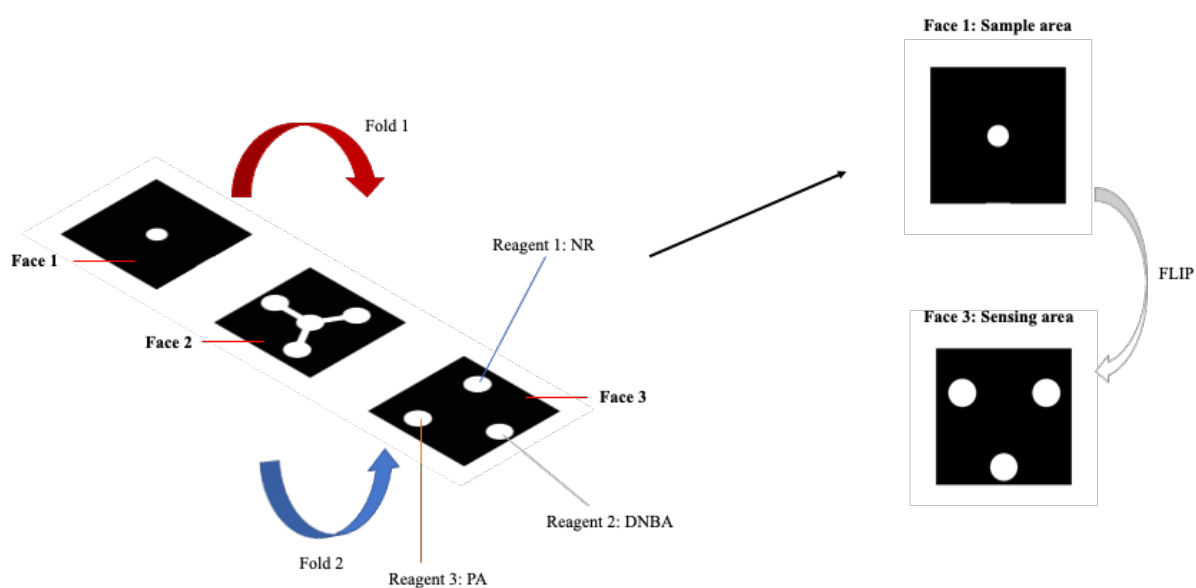


Fig 4.1 Schematic of origami  $\mu$ PAD.

This origami-paper-based device is used in this study for the determination of creatinine in urine samples

### 4.2.3 Analysis of samples

Two microliters of 5 M NaOH were spotted on one spot and allowed to dry for 2 minutes. Two microliters of 0.3 M DNBA in 0.45M NaOH were spotted onto the NaOH spot; two microliters of Nessler's reagent and picric acid mixture (0.04M in 2M NaOH) were subsequently spotted on the other two spots. The device was then dried for 2 ½ minutes and then fastened together with staples. Sixty microliters of the urine sample were spotted on Face 1 and the device was turned to reveal Face 3 after 30- 60 seconds depending on the viscosity of the urine sample.

A smartphone camera (iPhone 6, Apple Inc., Cupertino, CA, US) was used to record the image of the sensing part of the device. The evaluation of the interaction between creatinine and picric acid, 3,5-dinitrobenzoic acid and Nessler's reagent respectively was estimated by a deconvolution of the red, green and blue components using the ImageJ 1.53a software to obtain the RGB distance ( $\Delta RGB$ ) by the following equation:

$$\sqrt{(R - R_0)^2 + (G - G_0)^2 + (B - B_0)^2}$$

In the above equation, the values  $R_0$ ,  $G_0$  and  $B_0$  correspond to the components R, G and B of a saline solution, which was analysed for each test and considered as reference value. While the value R, G and B are the red, green and blue components of the sample area.

### 4.2.4 Validation

The validation parameters investigated were linearity, specificity, limit of detection (LOD), lower limit of quantification (LLOQ), upper limit of quantification (ULOQ), and within-run and between days precision and accuracy.

The linearities achieved for the reagents evaluated- Nessler's reagent, 3,5-dinitrobenzoic acid and Jaffé's reagent ranged from 0.02 to 0.2gL<sup>-1</sup>.

The specificity of the experiment was investigated by analysing potential interferences in urine. Trisodium citrate dihydrate, sodium chloride, ammonium chloride, calcium chloride, sodium oxalate and disodium hydrogen phosphate were all analysed to assess each of their colorimetric responses to each reagent.

The limit of detection (LOD) was defined as the lowest concentration at which a colorimetric response which could be discriminated from the saline solution by naked-eye observation on each one of three replicates and by using the smartphone recording. The lowest limit of quantification (LLOQ) was the lowest concentration of creatinine at which the RGB value recorded showed an accuracy and precision in the range of 25% (from three replicates for six runs). Conversely, the upper limit of quantification (ULOQ) was the highest concentration of creatinine at which the recorder RGB values met the same criteria.

The reproducibility and accuracy of the method was evaluated by analysing creatinine solutions at the LLOQ ( $0.02 \text{ gL}^{-1}$ ), ULOQ ( $0.2 \text{ gL}^{-1}$ ) and three intermediate concentrations ( $0.06$ ,  $0.1$  and  $0.15 \text{ gL}^{-1}$ ). Analysis was conducted on three replicates of each concentration for six consecutive days to assess the precision and accuracy of the method. Intra and inter precision within and between days were defined by the calculation of %RSD of the corresponding RGB values. The requirement of the validation criteria was that the %RSD values were less than 20%, with the requirement for LLOQ and ULOQ less than 25%. Accuracy was expressed as the percentage of the theoretical concentration experimentally measured in fortified samples with known concentrations of creatinine. An acceptable accuracy value was in the range 85–115%.

### 4.3 Results and Discussion

The present method explores three reagents for the quantitative detection of creatinine. The Jaffé's method, clinically adapted by Otto Folin in 1919 involves the reaction of creatinine with picric acid in an alkaline solution to produce a coloured complex as shown in the equation below:

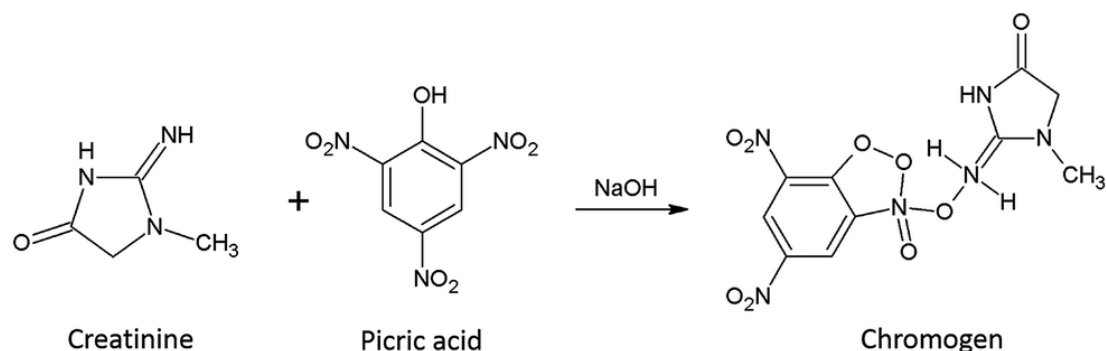


Fig 4.2 Reaction of creatinine and picric acid in NaOH resulting in characteristic yellow chromogen.

Although the Jaffé's method is widely used for clinical purposes, it is non-specific with interferences from several compounds including glucose, pyruvate and ascorbate. In 1936, three independent research groups- Langley and Evan, Bollinger and Behre- all proposed a procedure for the determination of creatinine with greater specificity using 3,5-dinitrobenzoic acid in an alkaline solution resulting in a purple complex as denoted in the following reaction:

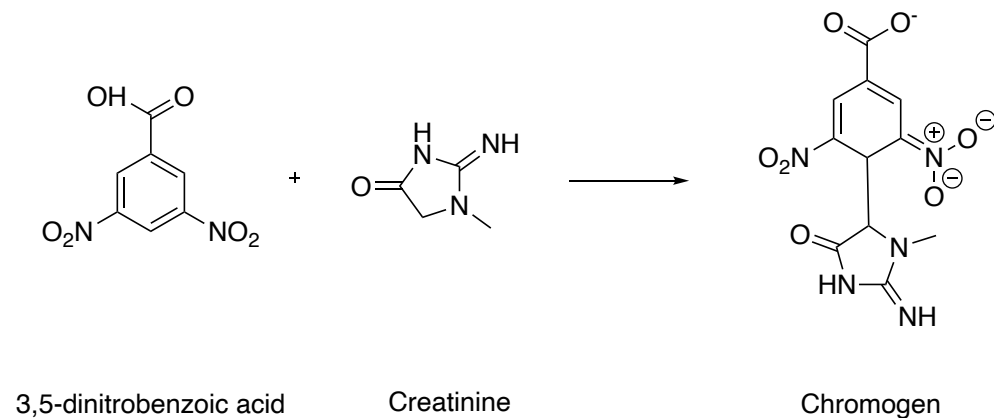


Fig 4.3 Reaction of creatinine and 3,5-dinitrobenzoic acid in NaOH resulting in characteristic purple chromogen

Nessler's Reagent which is primarily used for the detection of ammonia also shows reactivity with creatinine with a colour change unique to that of ammonia. The reactant species of Nessler's Reagent is the mercury (II) iodide ion. Creatinine comprises two amine groups which react with Nessler's Reagent in the following manner:

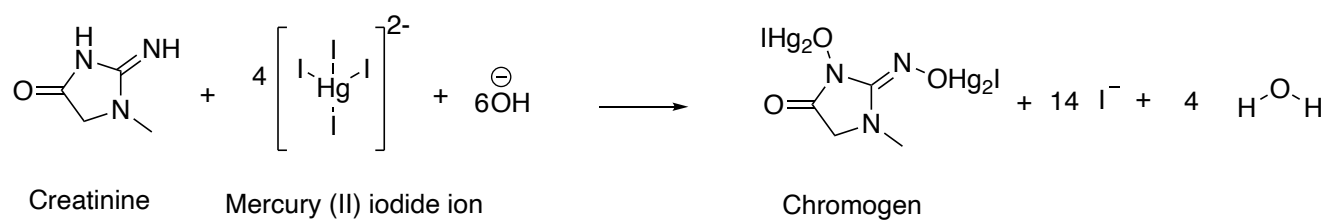


Fig 4.4 Reaction of creatinine and Nessler's reagent in NaOH resulting in yellow brown colour.

Creatinine is the by-product of muscle metabolism and is excreted in the urine. The determination of the concentration of urinary creatinine is a crucial parameter for assessing the validity of a urine sample for the detection of drugs of abuse. Due to the consequences of a positive drug test (termination from employment, criminal charges, fines, etc.), individuals may be inclined to adulterate their urine sample by utilizing various approaches. One of the most common techniques is by the intentional consumption of excess fluid in a relatively short period of time in an effort to dilute their urine. This can result in the drug being detected below the positive cut-off concentration resulting in false negative drug tests. To circumvent this problem, the preliminary step for the analysis of drugs of abuse involves the determination of the concentration of creatinine and is well established by forensic scientists and stated in [ref book]. One critical point is set at less than 20 mg/dL (0.2 g/L) and the second is less than or equal to 2 mg/dL (0.02 g/L). These creatinine concentrations, along with a corresponding specific gravity level, are used to determine if a urine sample is dilute or substituted as it is not consistent with clinical characterisations of normal human urine [71].

#### 4.3.1 Design and validation of the microfluidic paper-based device

The linearity of the method for all reagents was tested in the range of 0.02 to 0.2 gL<sup>-1</sup>, with limits of detection and limits of quantification of 0.02 gL<sup>-1</sup>.

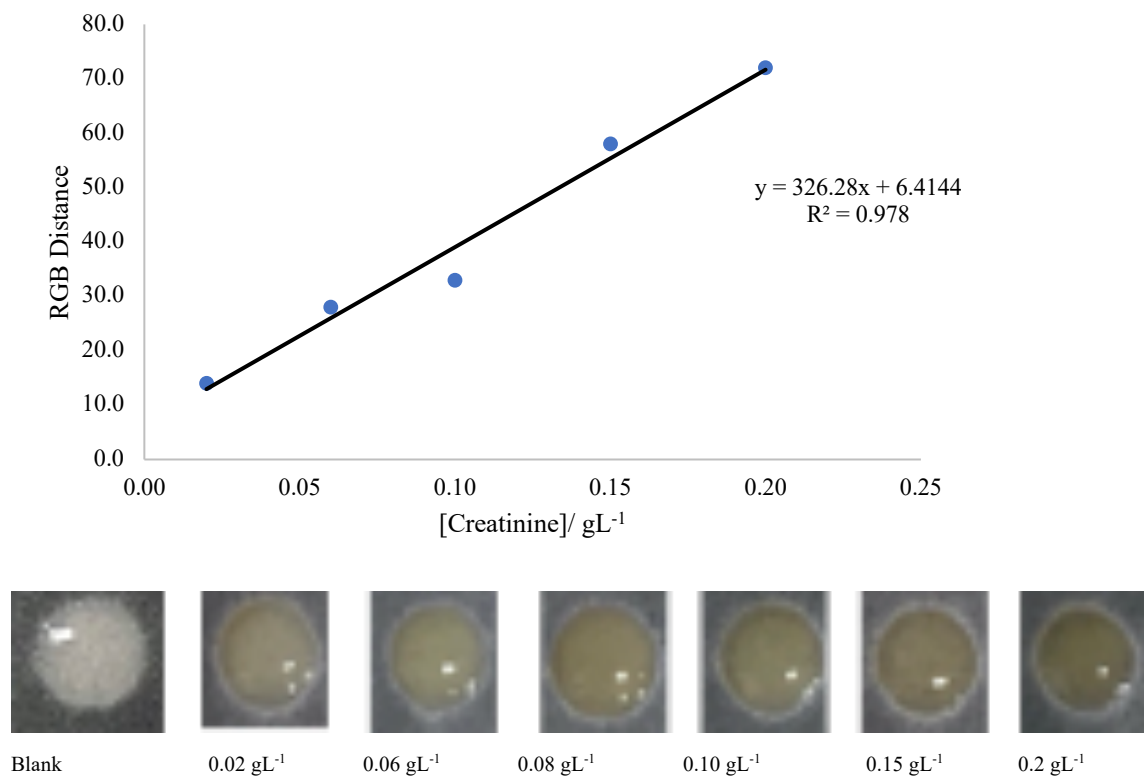


Fig. 4.5 Linearity and optical images of increasing creatinine concentration interaction with Nessler's reagent

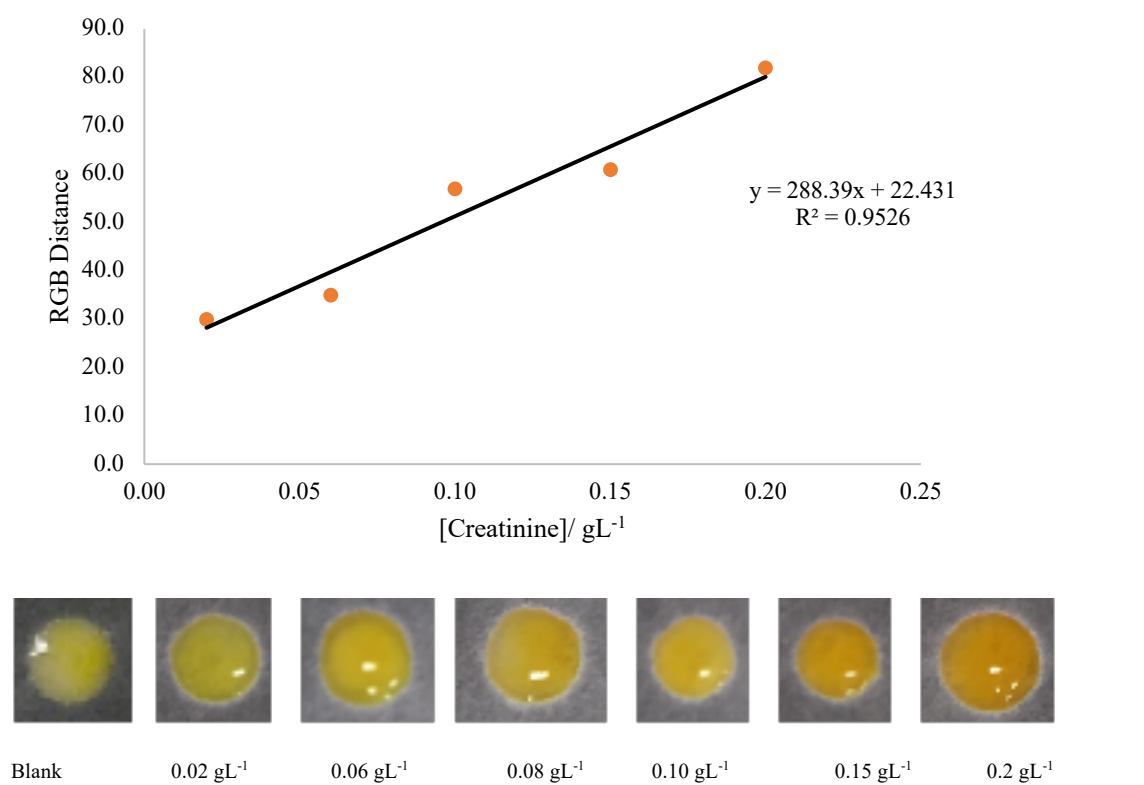


Fig. 4.6 Linearity and optical images of increasing creatinine concentration interaction with picric acid solution

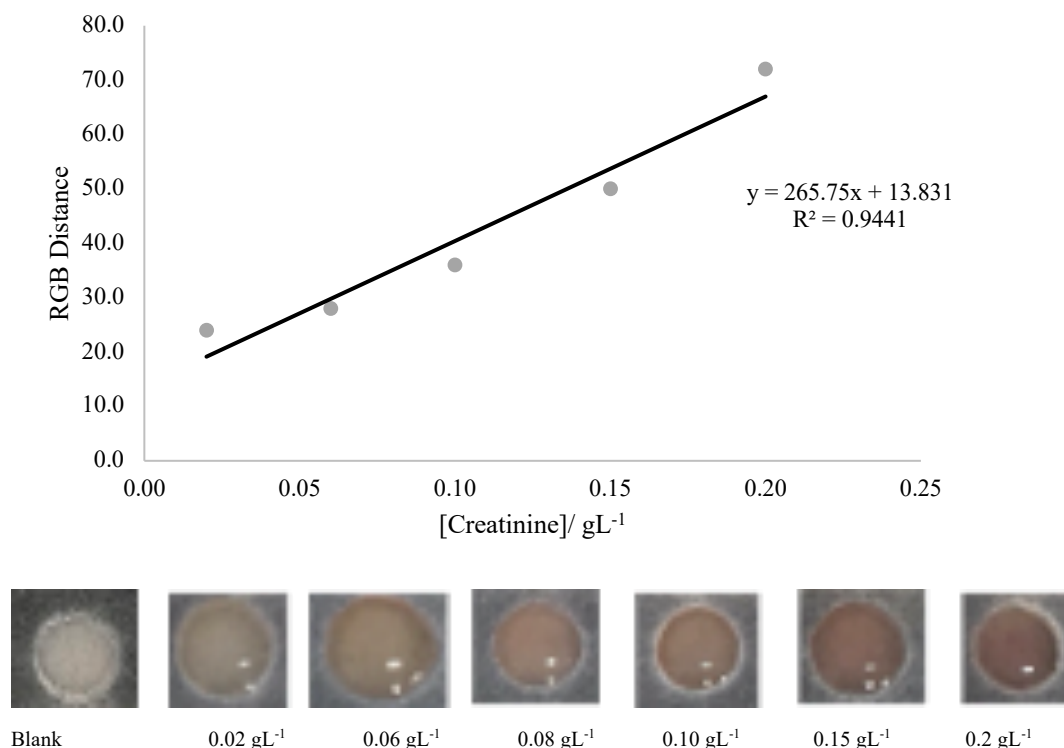


Fig. 4.7 Linearity and optical images of increasing creatinine concentration interaction with DNBA solution

The %RSD of within-run and between days precision were evaluated using the LLOQ, three intermediate points and ULOQ of the calibration curve (0.02, 0.06, 0.1, 0.15, 0.2 gL<sup>-1</sup> respectively). Within-run and between days precision in addition to accuracy were satisfactory, with at least 75% of calibrator levels showing differences in the nominal concentration within  $\pm 25\%$  for the lowest (LLOQ) and the highest (ULOQ) calibrator level, while it was within  $\pm 20\%$  for the other calibrator levels.

The selectivity of the procedure was assessed by testing various substances commonly found in urine including urea, MgSO<sub>4</sub> NaCl, CaCl<sub>2</sub>, KCl, Na<sub>2</sub>HPO<sub>4</sub>, NH<sub>4</sub>Cl, Na<sub>2</sub>C<sub>2</sub>O<sub>4</sub> and Na<sub>3</sub>C<sub>6</sub>H<sub>5</sub>O<sub>7</sub> [72]. For simplification, only the reagent and analytes which gave a colorimetric response are included in Fig 4.8. The RGB distance for NH<sub>4</sub>Cl and urea are both significantly lower than the LOD of the reaction and so, can be considered negligible. It is therefore reasonable to

conclude that the proposed method is selective for the determination of creatinine in urine samples.

Both the limit of detection (LOD) and lowest limit of quantification (LLOQ) were determined as  $0.02 \text{ gL}^{-1}$  for this method. This was qualified with the determination of the accuracy and precision of this value within 75- 125% and  $\leq 25\%$ , respectively.

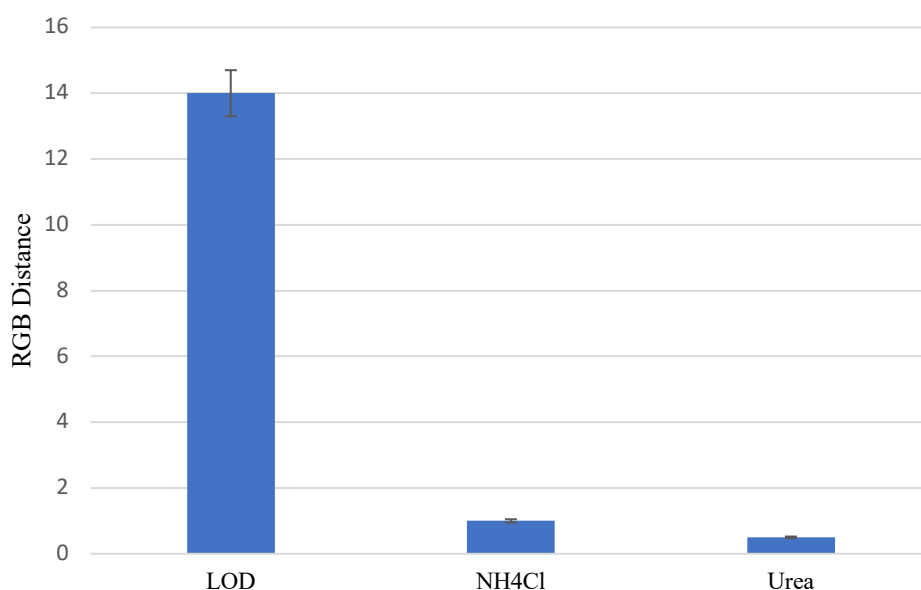


Fig 4.8 Specificity studies

The colorimetric response to common components of urine was investigated with only Nessler's reagent showing a slight change in RGB distance for  $\text{NH}_4\text{Cl}$  and urea. The RGB distance for  $\text{NH}_4\text{Cl}$  and urea are both significantly lower than the LOD of the reaction and so, can be considered negligible. It is therefore reasonable to conclude that the proposed method is selective for the determination of creatinine in urine samples.

#### 4.3.2 Optimisation studies

It was imperative to first establish the concentrations of the reagents that would be used. The main challenge with optimising the concentrations was the solubility of the organic compounds 3,5-dinitrobenzoic acid and picric acid in NaOH. As previously discussed, an alkaline environment is required for the reaction to proceed and so this was crucial. In order to determine the colorimetric reagent solution with picric acid, 0.01, 0.02, 0.03, 0.04 and 0.05 M of picric acid solution and 2 M NaOH solution was mixed in an Eppendorf tube. Subsequently,

as the picric acid solution of 0.04 M showed the best solubility, it was fixed at 0.04 M and the NaOH concentrations were varied at 1, 2, 3, 4 and 5 M. The combination of 0.04 M picric acid in 2 M NaOH showed the best solubility and so this was used. For 3,5-dinitrobenzoic acid (DNBA), using data presented by Behre [66], it was established that the optimal ratio of DNBA to NaOH was 1:1.5. However, through investigations, it was noted that this does not work well with high concentrations of DNBA, and the optimal concentration found, which is used in this procedure, is 0.3 M DNBA in 0.45 M NaOH. This reagent concentration was obtained by evaluating concentration levels of DNBA at 0.3, 0.5, 1 and 2 M with their respective NaOH concentrations based on the established ratio. Notably, the addition of 2 $\mu$ L of 5M NaOH to the DNBA spot on the device produced more vivid colours. Nessler's reagent did not require any preparation and was used directly.

The effect of temperature on the resultant colour change was also investigated at temperatures 4, 21 and 35 °C at two concentrations of creatinine (0.15 and 0.2 gL<sup>-1</sup>). No significant difference was recorded, which is positive for potential use in the field when temperatures cannot be controlled.

Finally, the stability of the reagents was also examined at two creatinine concentrations (0.15 and 0.2 gL<sup>-1</sup>). The device showed consistent reactivity until up to one month stored at 4 °C, after which, the picric acid and Nessler's reagent showed low reactivity and the DNBA colour change was notably different from what has been consistent in the past experiments.

#### 4.3.3 Analysis of real samples

The practicability of this method's use as a preliminary step in the quantification of drugs of abuse was evaluated by testing 13 urine samples with known concentrations obtained from the immunoassay method. These samples had creatinine concentrations between 0.025 and 0.135 gL<sup>-1</sup>.

The relationship between the urinary creatinine concentrations determined by the immunoassay method and the proposed methods- i.e., Nessler's reagent, picric acid and 3,5-dinitrobenzoic acid are denoted below:

- (i) Nessler's reagent:  $y=4.1065x$  [ $R^2= 0.8971$ ]
- (ii) Picric acid:  $y= 1.124x$  [ $R^2= 0.9153$ ]
- (iii) 3,5- dinitrobenzoic acid:  $y= 5.6252x$  [ $R^2= 0.9438$ ]

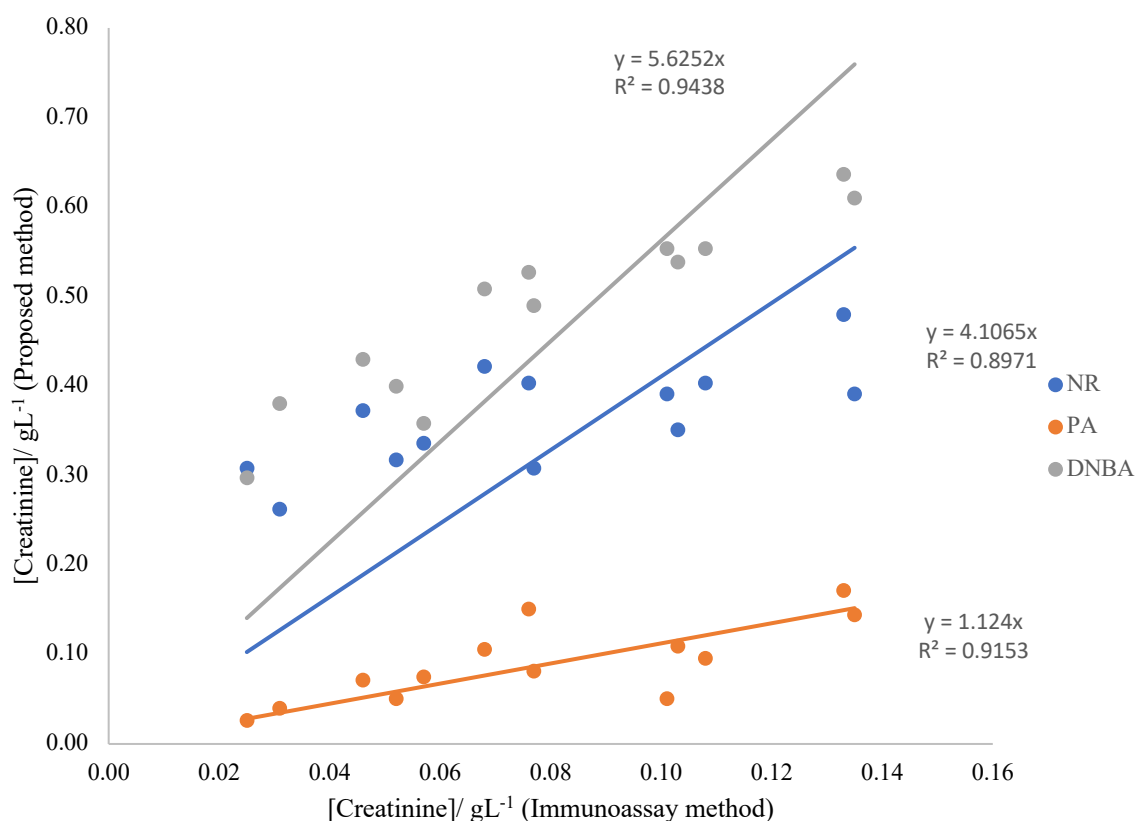


Fig. 4.9 Correlation between immunoassay and  $\mu$ PAD method

Correlation between creatinine concentration of immunoassay method (x-axis) and creatinine concentration of proposed methods (y-axis)- with Nessler's reagent (blue), PA (orange) and DNBA (grey)

Although the Jaffe's method, employing picric acid, is the gold standard for the determination of creatinine in urine samples using immunoassays, its transfer onto a paper platform was not the most successful of the three methods. DNBA ( $R^2=0.9438$ ) seems more suitable when compared to picric acid ( $R^2=0.9153$ ) and Nessler's reagent ( $R^2=0.8971$ ).

Nessler's reagent is not a specific reagent for creatinine and so the results are justified.

For simplicity, the correlation between the RGB distance, acquired after image analysis, and the known creatinine concentrations were evaluated.

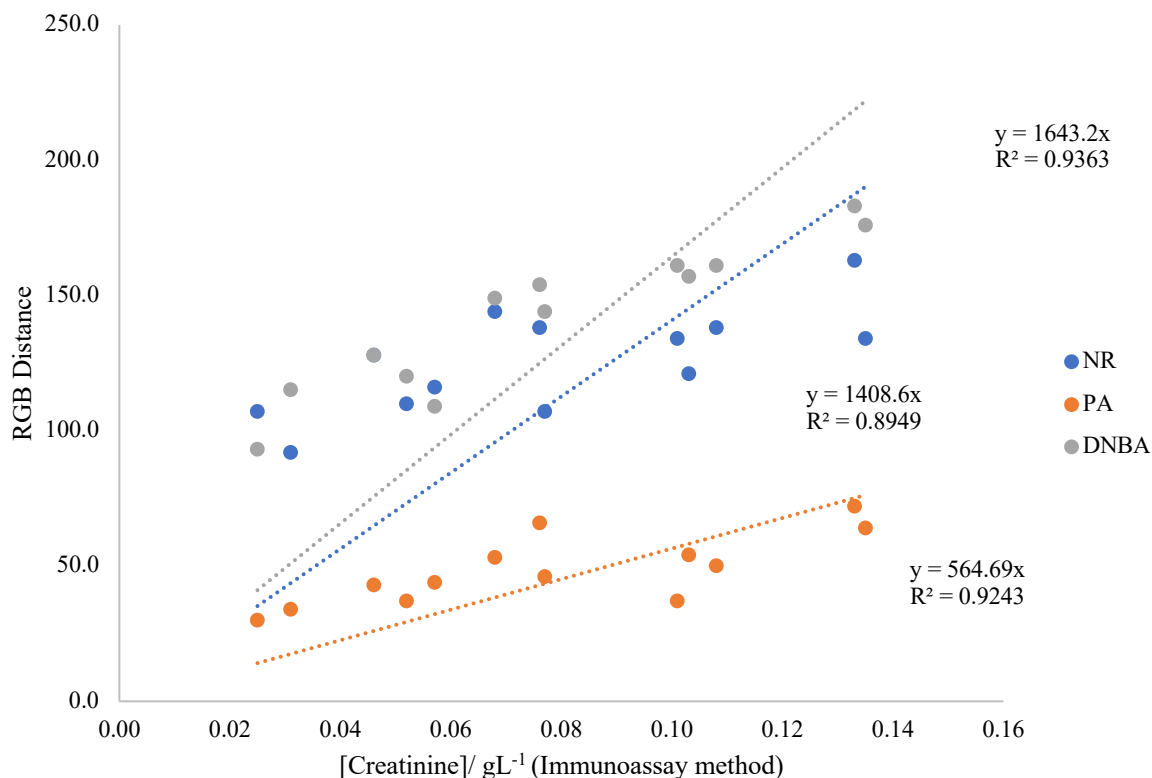


Fig. 4.10 Correlation between immunoassay and RGB distance

Correlation between Immunoassay method (x-axis) and RGB distance of proposed methods (y-axis)- with Nessler's reagent, PA and DNBA

#### 4.4 Conclusion

The development of this paper-based microfluidic device introduces a cost-effective, rapid, user-friendly and simple method for the determination of urinary creatinine which is imperative in all drug screening analysis. The tool also uses a simple detection and data treatment

technique, which may be useful at the point-of- need, or in remote areas where immunoassays are not available. The measurement of the RGB distance, which can be measured by the deconvolution of the colour of the sensing regions, can be done using common free apps for smartphones like “What a colour”. This RGB distance is correlated with the urinary creatinine concentrations, which is necessary to determine whether a urine sample is viable for the next stage of drug screening.

#### 4.5 Future research

More samples can be tested to establish a greater data set.

## 5. THE DEVELOPMENT OF A PAPER-BASED MICROFLUIDIC DEVICE CAPABLE OF CONDUCTING RECOMBINASE POLYMERASE AMPLIFICATION (RPA) FOR THE DETECTION OF CARBAPENEMASES.

Prior to the mass production of antimicrobials, the estimated average lifespan varied globally from 28.1 years in Asia to 46.8 years in Europe [73]. In 1900 the most common cause of mortality was attributed to untreatable bacterial infections which accounted for a third of all documented deaths [74]. The synthesis of Prontosil [75] and penicillin V [76] in 1936 and 1943, respectively marked the beginning of the antimicrobial golden age in which thousands of natural and synthetic antimicrobials were discovered and developed. Each antimicrobial is grouped together in classes, of which, beta-lactams are the largest, and includes the subgroup carbapenems.

Although the advent of antimicrobials dramatically reduced death rates, the accelerated exposure of bacteria to antimicrobials by medical prescriptions has caused bacteria to develop antimicrobial resistomes. Beta-lactams are the most widely prescribed antibiotics, causing a significant increase in bacterial resistance against them. Patients whose infections are resistant against extended-spectrum beta-lactams are prescribed carbapenems as a last resort.

Globally, the number of carbapenem prescriptions has increased yearly, leading to the production of carbapenemases by bacteria, enzymes capable of hydrolysing carbapenems. These bacteria therefore develop antimicrobial resistance (AMR) against carbapenems. Five carbapenemases, referred to as the 'big five', have been identified as the most concerning threat to the worldwide propagation of AMR, including the Verona integron-encoded metallo- $\beta$ -lactamase (VIM).

VIM poses a particularly alarming problem as some pathogens encoding variants of VIM have shown resistance to aztreonam, a new antibiotic used to treat severe infections, meaning that they may be acquiring resistance to all antibiotics [77]. The identification and subsequent quantification of VIM requires several intricate procedures, noteworthily, the use of the Polymerase Chain Reaction (PCR) for molecular diagnostics. This technique, however, has disadvantages which have limited its global application. These include the requirement of expensive laboratory-based equipment, the necessity for high temperature thermal cycling –

ranging from 60°C to 94°C [78, 79] and skilled personnel to operate. In an effort to increase the speed and accessibility of nucleic acid amplification techniques, research into the development of ASSURED point-of-care devices emerged.

Isothermal amplification is a method of DNA amplification which is performed at a single temperature. This method reduces costs, negates the use of centralised equipment, and increases the amplification rate. Recombinase Polymerase Amplification (RPA) is a type of isothermal amplification that has quicker reaction times when compared to PCR but is the only method that has a limit of amplification comparable to PCR. Briefly, RPA utilises the enzyme recombinase to drive amplification, along with specifically designed forward and reverse primers, optimally between 37-42 °C. A reporter probe, specific to the desired detection method, is added after RPA amplification. Many papers have successfully combined RPA with instrumentation-free readout systems such as lateral flow strips [80-82]. RPA's ability to amplify nucleic acids at low temperatures, reduces the need for equipment thus reducing costs. The added feature of low-cost readout systems makes RPA a promising amplification technique for the implementation in point-of-care tests (POCTs).

The goal of this study is the development of an ASSURED POCT which incorporates RPA amplification and a readout with a handheld SERS reader to detect VIM (of the “big five” carbapenemases). So far, the research group has designed and sequenced forward and reverse primers and a suitable reporter probe for the target molecule- VIM DNA template. With this, they have successfully conducted RPA of VIM on specific, inexpensive magnetic beads in a 96-well plate. Magnetic beads can be used as a platform to capture and extract analytes from clinical samples. They are usually nm to  $\mu\text{m}$  in size, with an iron or cobalt core and inorganic or polymeric surface that can be easily functionalised [83]. This functionalised surface is what target molecules are bound to (Fig. 5.1). Additionally, magnetic beads are robust and can be paired with a wide range of detection methods including SERS. Surface Enhanced Raman Spectroscopy (SERS) is a powerful technique that is able to provide structural information about molecules with high detection sensitivity. As part of this study, a handheld SERS reader is being developed for detection. For accurate detection, the analyte/ target molecule must be in solution. Although the reaction was successful in a 96-well plate, this platform is not suitable as a POCT and so, the use of a paper-based microfluidic device was proposed. A device design with its hydrophilic sensing/reaction area and hydrophobic barriers, can easily create or mimic

the well design of the plate. Ultimately, my role in this study was the preliminary evaluation of the transfer of the RPA reaction onto a paper platform.

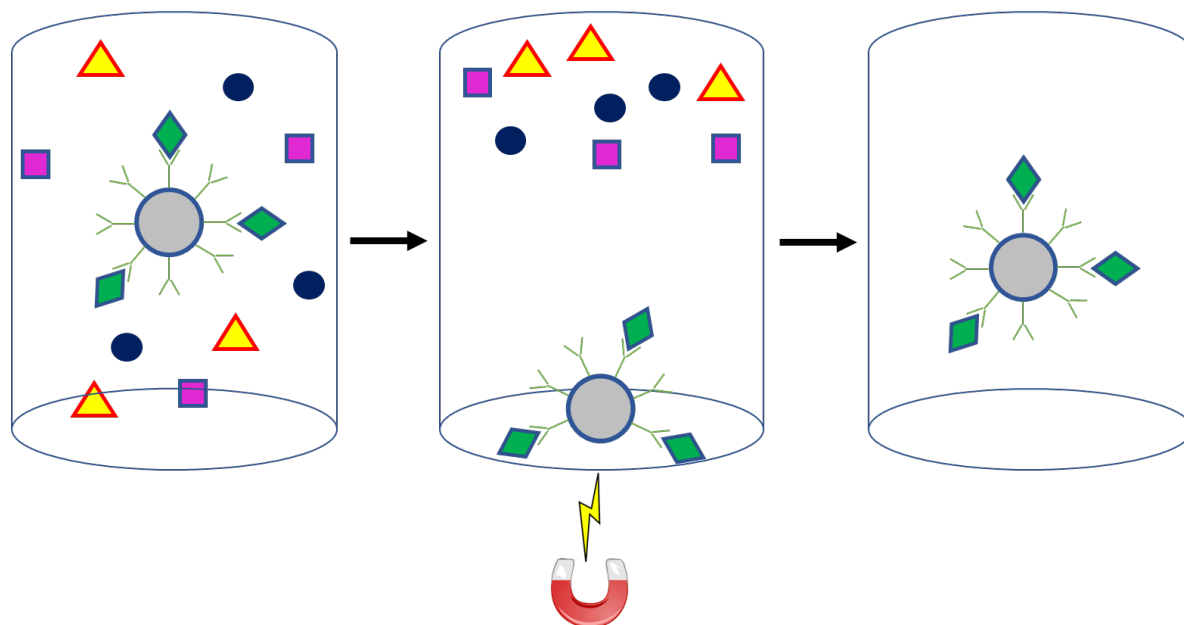


Figure 5.1: Schematic diagram of magnetic beads application to extract target analytes. The figure shows the process of analyte extraction using magnetic beads. The magnetic bead in grey/blue are functionalised with a ligand (green antibody), the ligand binds the target analyte (green/blue diamond), when a magnet is applied, the magnetic bead is attracted to the base whilst non-target constituents can be removed leaving only the target analyte bound to the magnetic bead.

## 5.1 Materials and Methods

This section highlights solely the aspects of the study that involved the fabrication and use of the paper-based microfluidic device. A more detailed account of the experimental can be found in the Appendix.

### 5.1.1 Chemicals and Materials

Trimethoxymethylsilane (MTMS), HCl and NaOH were all purchased from Thermo Fisher Scientific. Tween 20 and the components of PBS buffer- KCl,  $\text{KH}_2\text{PO}_4$ ,  $\text{Na}_2\text{HPO}_4$  and NaCl were all bought from Sigma Aldrich. The RPA kit, TwistAmp Liquid basic kit was purchased from TwistDX and the magnetic beads from Ocean Nanotach. KPL sureblue TMB (3, 3', 5, 5'-tetramethylbenzidine) microwell peroxidase substrate was purchased from Seracare.

### 5.1.2 Design and 3D printing of template unit

The template unit comprises three components- a holder (which fits the three templates), three templates and a base (which holds the paper substrate). This template is designed to create the hydrophilic area of the device. The template comprises a square base ( $l=2.5$  cm,  $h = 0.9$ cm) with a cross, creating four quadrants, as well as a cylinder running through the centre. One portion of the cylinder is longer than the other. The shorter part, denoted by  $s$  ( $h = 0.3$ cm,  $d = 0.5$ cm) on the illustration is used to create the hydrophilic area on the device. This slight elevation is important to allow for the depositing of sol gel onto the paper substrate (in the base). The longer part,  $f$  ( $h = 0.7$ cm,  $d = 0.5$  cm), is inserted into the holder (Fig. 5.2). The holder ( $l = 8.3$  cm x  $w = 3.5$  cm,  $h = 1.0$  cm) has an internal area of  $7.5$  cm x  $2.5$  cm. This internal area contains three cylindrical holes, the same height but a diameter ( $0.55$  cm) a little larger than that of  $l$ , equidistant from each other, to fit three templates at once. On the perimeter of the holder, six screw holes are included. Finally, the base has the same external dimensions as the holder, with an internal volume of  $l = 7.5$  cm,  $w = 2.5$  cm and  $h = 0.9$  cm. This internal volume fits the templates, and the perimeter includes six screw holes which align with the holder.

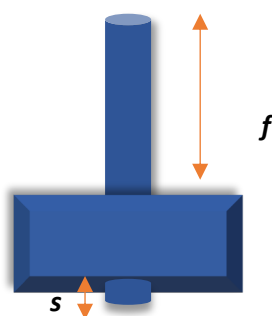
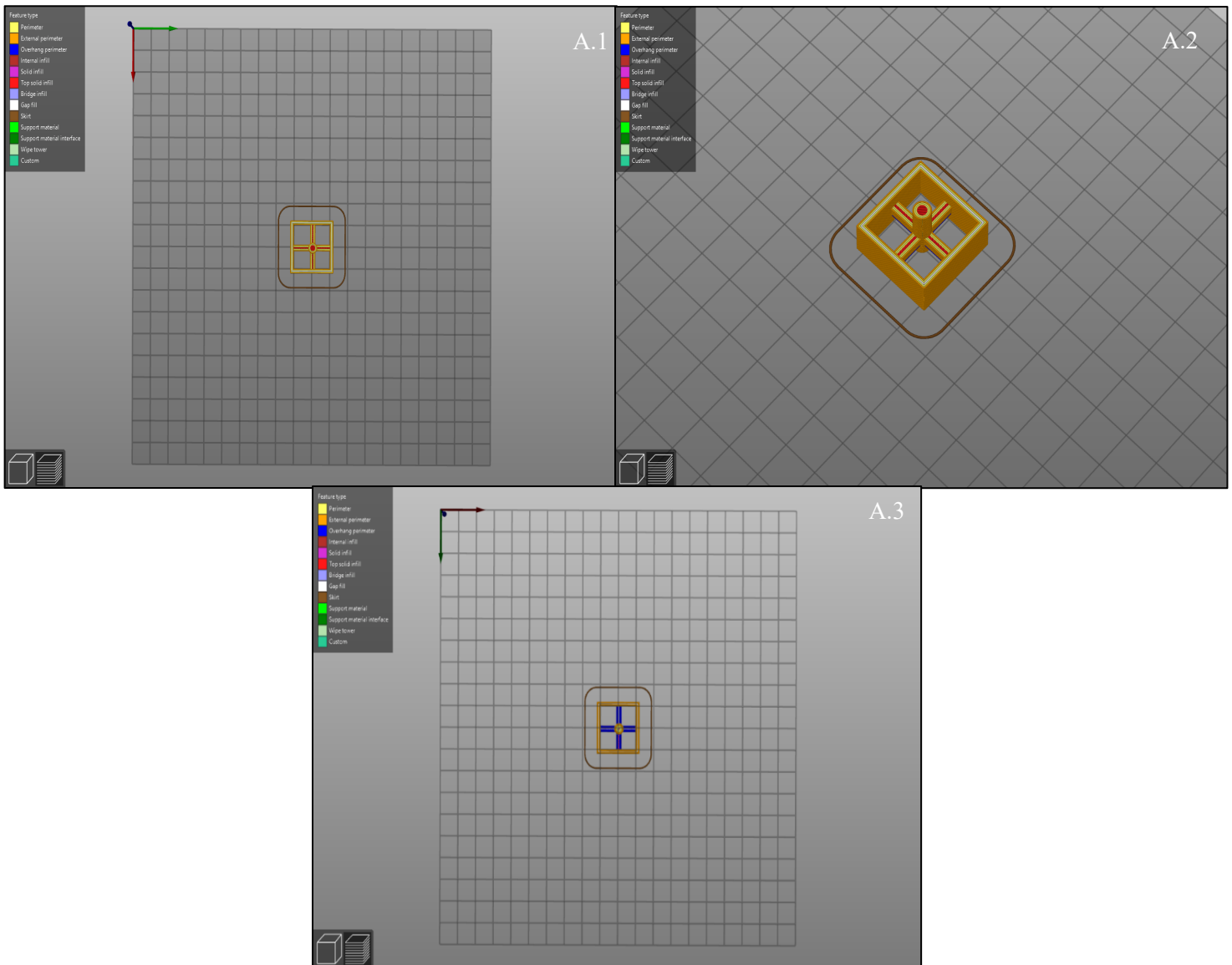


Fig. 5.2 Illustration of template

The fabrication of the template unit utilised an inexpensive, high-definition open-source Fuse Deposition Modelling (FDM) 3D printer (Original Prusa i3 MK3 by Josef Prusa, Prague, CZ). A dimensioned Computer-Aided Design of each of the three components was first created using Autodesk Fusion 360 software, then converted to STL format. The STL files were uploaded to PrusaSlicer, used to slice the 3D models to prepare them for 3D printing (Fig. 5.2). They were printed with 50  $\mu\text{m}$  resolution using Prusa Polylactic Acid (PLA) filament.



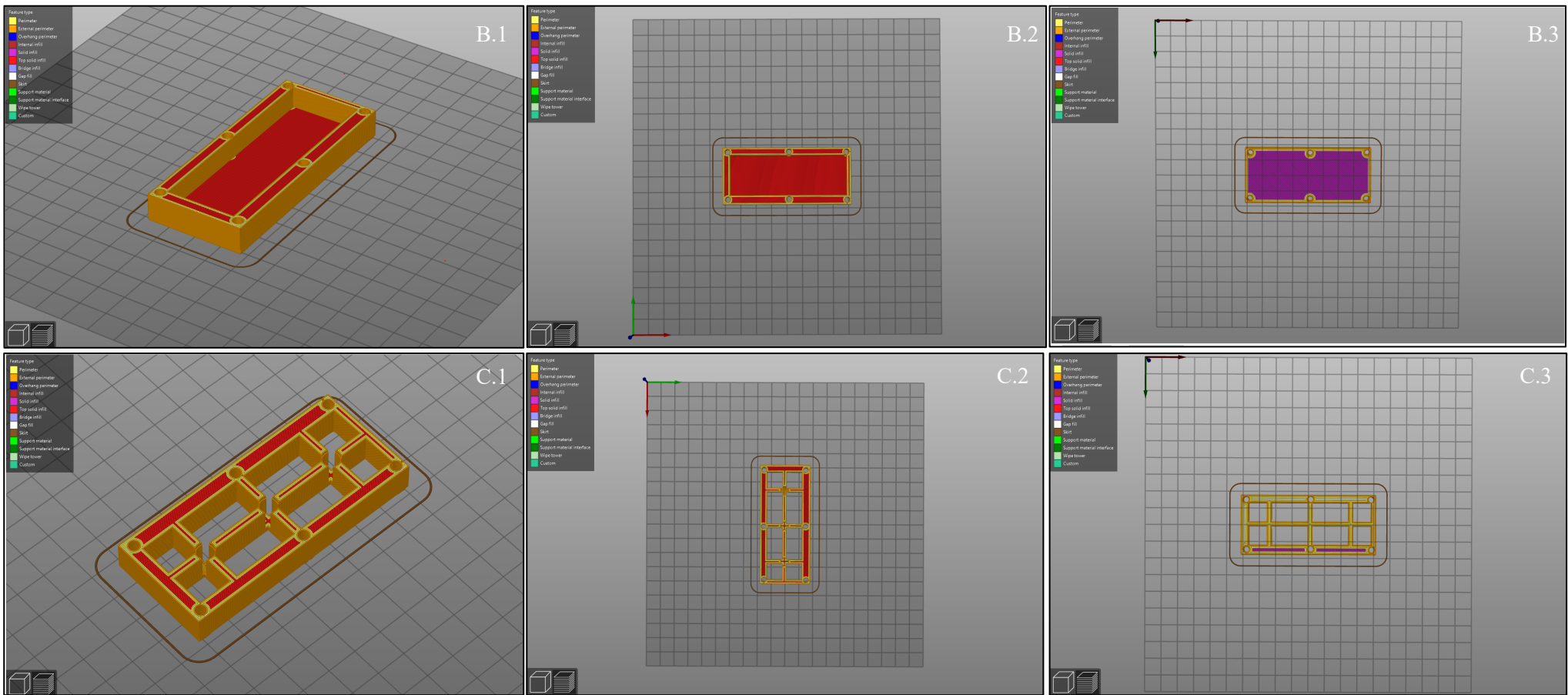


Fig. 5.3 PrusaSlicer images of components of template unit.

A.1, A.2 and A.3 depict the xy, orthogonal (xyz) and yx views of the template, respectively. B.1, B.2 and B.3 are images of the orthogonal, xy and yx views of the base of the template unit and lastly, C.1, C.2 and C.3 illustrate the orthogonal, xy and yx views of the holder.

### 5.1.3 Fabrication of device

To make the sol gel, 0.1M HCl and trimethoxymethylsilane (MTMS) (1:4 v/v) were mixed and sonicated in an ice bath for 1h. Whatman #1 paper was inserted into the holder, the templates placed and covered, then secured with cap screws, washers and nuts. Fifteen microliters of sol gel were added to each quadrant and allowed to dry (~ 20 mins).

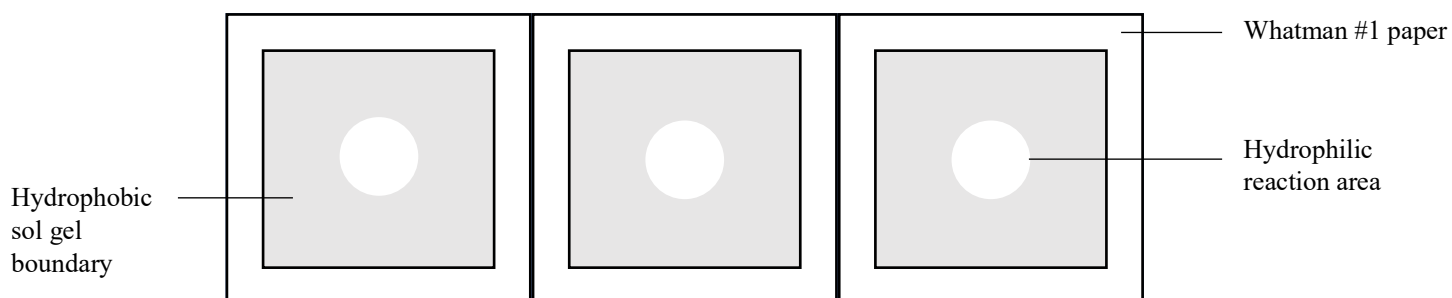


Fig. 5.4 Schematic of resultant paper-based microfluidic device

### 5.1.4 RPA on paper

Once the device is dried, ten microliters of primed beads were added to the spot and allowed to dry. Thirty microliters of the RPA mixture with VIM DNA template and MgOAc were added to the dried spot and the solution mixed by pipetting until uniform. RPA was conducted at 37 °C for 35 mins. The spot was then cut out and added to a low-capacity binding Eppendorf and washed with x1 PBS, 0.05% Tween buffer three times. The reporter probe was added, vortexed and left for an hour at RTP. The final step consisted of the RPA method was UV detection using 3,3',5,5'-Tetramethylbenzidine (TMB) as the chromogenic substrate. The paper was removed and placed in a separate Eppendorf where TMB was added and vortexed. The resultant solution was transferred to a well plate for UV analysis @ 630nm. The reactions were performed in triplicate

## 5.2 Results and Discussion

The main challenge for the conversion of this assay onto a paper-based microfluidic device was the issue with the hydrophobic barriers. The traditional hydrophobic wax proved to be susceptible to the strong detergents in the RPA solution and was easily compromised. A preliminary evaluation was conducted to determine whether sol gel could be a possible replacement, as in literature, it shows great resistance against chemically aggressive solvents [28].

### 5.2.1 Optimisation studies for sol gel and paper substrates

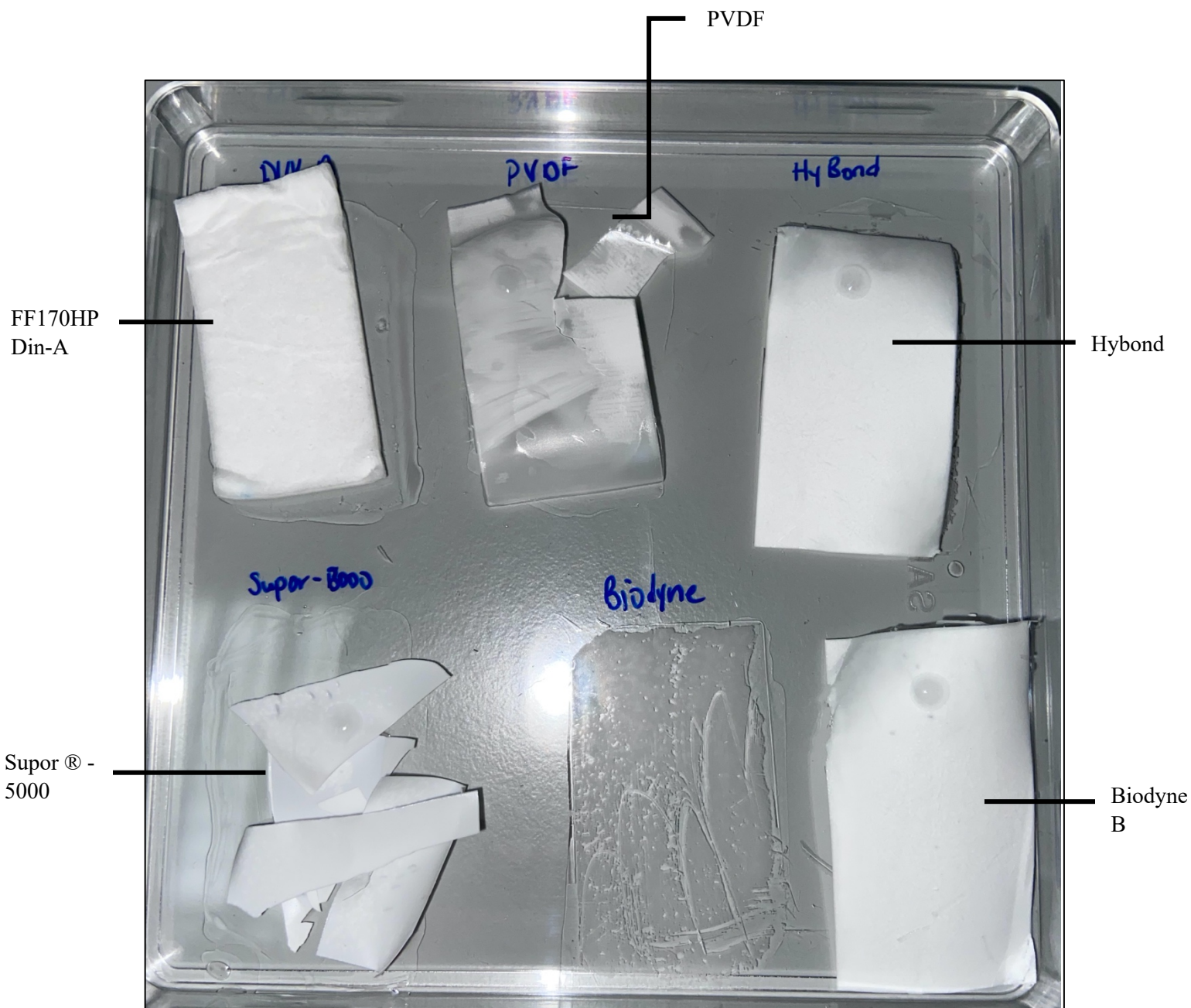
In a similar manner to wax printing, an inkjet printer was proposed to produce the paper-based microfluidic device. The viability of sol gel as an ink and NaOH as an etching agent was evaluated.

Firstly, six types of paper substrates were assessed by dipping 2 cm x 4 cm paper strips into the sol gel solution (MTMS and 0.1M HCl 4:1 v/v), prepared according to the protocol by Wang et al [28]. The paper substrates were Whatman #1 filter paper and nitrocellulose-type papers including FF170HP Din-A, PVDF, Supor®-5000, Biotodyne B and Hybond. Although the inert surface of Whatman #1 chromatography paper has proven favourable for most applications in forensic science [1], nucleic acid assays typically required a charged surface. This is because DNA is negatively charged and so, the positively charged surfaces of nitrocellulose-type paper are usually used, as evident in most lateral flow devices [7]. Nitrocellulose is formed from the nitration of cellulose. In addition to the type of polysaccharide which constituted each paper, they also varied in pore size from 0.2 to 11 µm (Table 5.1).

*Table 5.1: Paper substrates evaluated for sol gel dipping with their corresponding polysaccharide type, pore size and charge.*

NAME	TYPE OF POLYSACCHARIDE	PORE SIZE/ µm	CHARGE
Whatman #1	cellulose	11	0
FF170HP Din-A	nitrocellulose	0.45	+
PVDF	nitrocellulose	0.2	+
Supor®-5000	nitrocellulose	5.0	+
Biotodyne B	nitrocellulose	0.45	+
Hybond	nitrocellulose	0.2	+

The suitable paper substrates were determined by the impenetrability of the paper strip to the addition of a 10 mL droplet of RPA solution. Of the seven paper substrates tested, three were viable- Whatman #1, Biodyne and Hybond for the next stage of experimentation. PVDF and Supor®-5000 were more lightweight making the paper brittle and FF170HP Din-A became hard and non-malleable after sol gel impregnation (Fig 5.4).



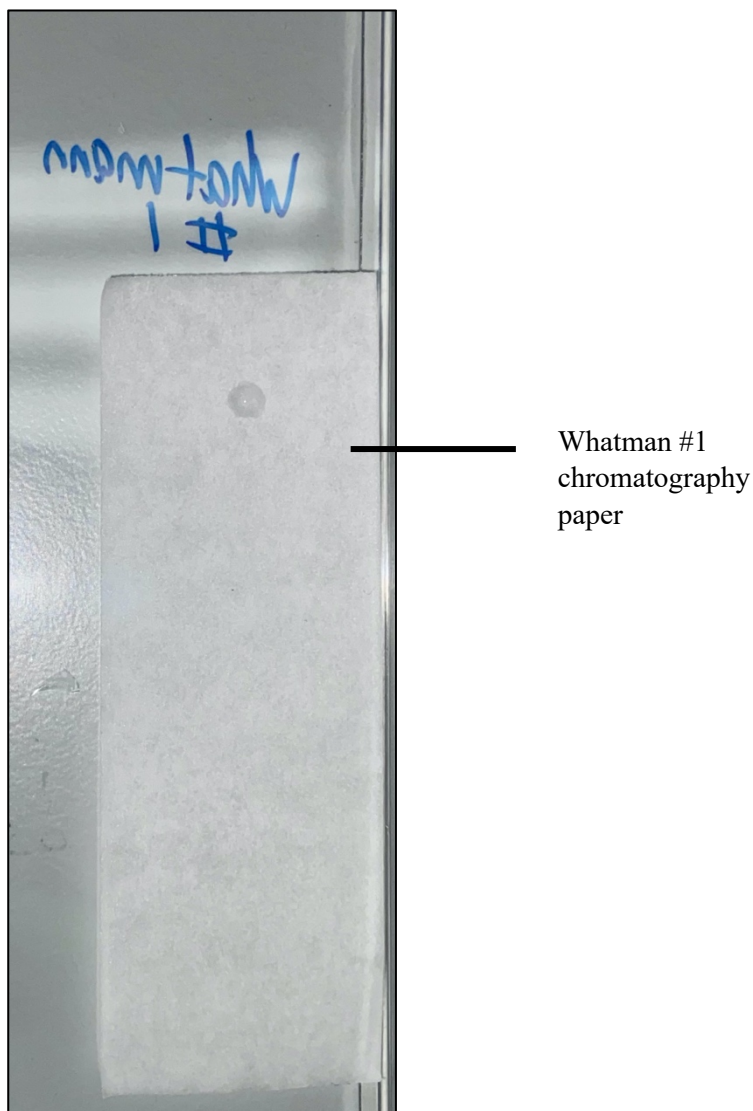


Fig 5.5 Results of sol gel impregnation studies

The chemically aggressive RPA assay was spotted on each paper strip to demonstrate their impenetrability. FF170HP DIN-A absorbed the assay immediately, proving that the impregnation was not successful. Supor ®-5000 and PVDF, although the hydrophobicity of the surface is evident, the process made them brittle. Hybond, Biodyne B and Whatman #1 chromatography paper were concluded to be viable.

Once the initial sol gel impregnation procedure proved successful, the effect of the HCl concentration on the stability of the gel was assessed. Results showed that the lower the concentration of HCl, the more stable the gel-less likely to solidify- in a glass bottle, but also the less hydrophobic. On this basis, after testing concentrations of 0.0001, 0.001, 0.01 and 0.1M

HCl, 0.001M HCl served as a good compromise between the shelf life of the gel and its hydrophobicity on paper.

Varying concentrations of 10, 2.0, 1.0, 0.5, 0.25 and 0.1 M NaOH were investigated for etching, with 2.0 M being the best suited. The etching process involved the spotting of 5  $\mu$ L of 2 M NaOH onto the impregnated and left for 15 minutes. The paper strip was then placed in 0.01 M HCl for 5 mins to neutralise. It was subsequently placed in water for 5 minutes then allowed to dry.

This method, however, was not used in the final fabrication of the  $\mu$ PAD as the use of an inkjet printer to produce the pattern was not successful. Sol-gel was injected carefully into the black ink cartridge for HP Officejet Pro 8600 Plus and printing was attempted on the pre-established three paper substrates. Only Whatman #1 proved sturdy enough to withstand several passes (6) through the printer, however, with every pass, the resolution of the channels became lower. Additionally, the sol gel boundaries showed no hydrophobicity meaning that the volume deposited in the multiple runs was not significant enough to absorb into the paper substrate.

### 5.2.2 3D printed template

From the knowledge of the use of templates for patterning [84], the possibility of creating a template via 3D printed modelling was explored. Since the sol gel was to be deposited by pipetting to create the hydrophobic boundaries, the template was created to design the hydrophilic area of the device. Fig 5.5

When trying to use the template unit, the pore size affected how quickly the sol gel flowed and so the smaller pore sizes of 0.2 and 0.45 for Hybond and Biodyne B respectively were not conducive to form the desired pattern. Whatman #1 paper was selected for further studies.

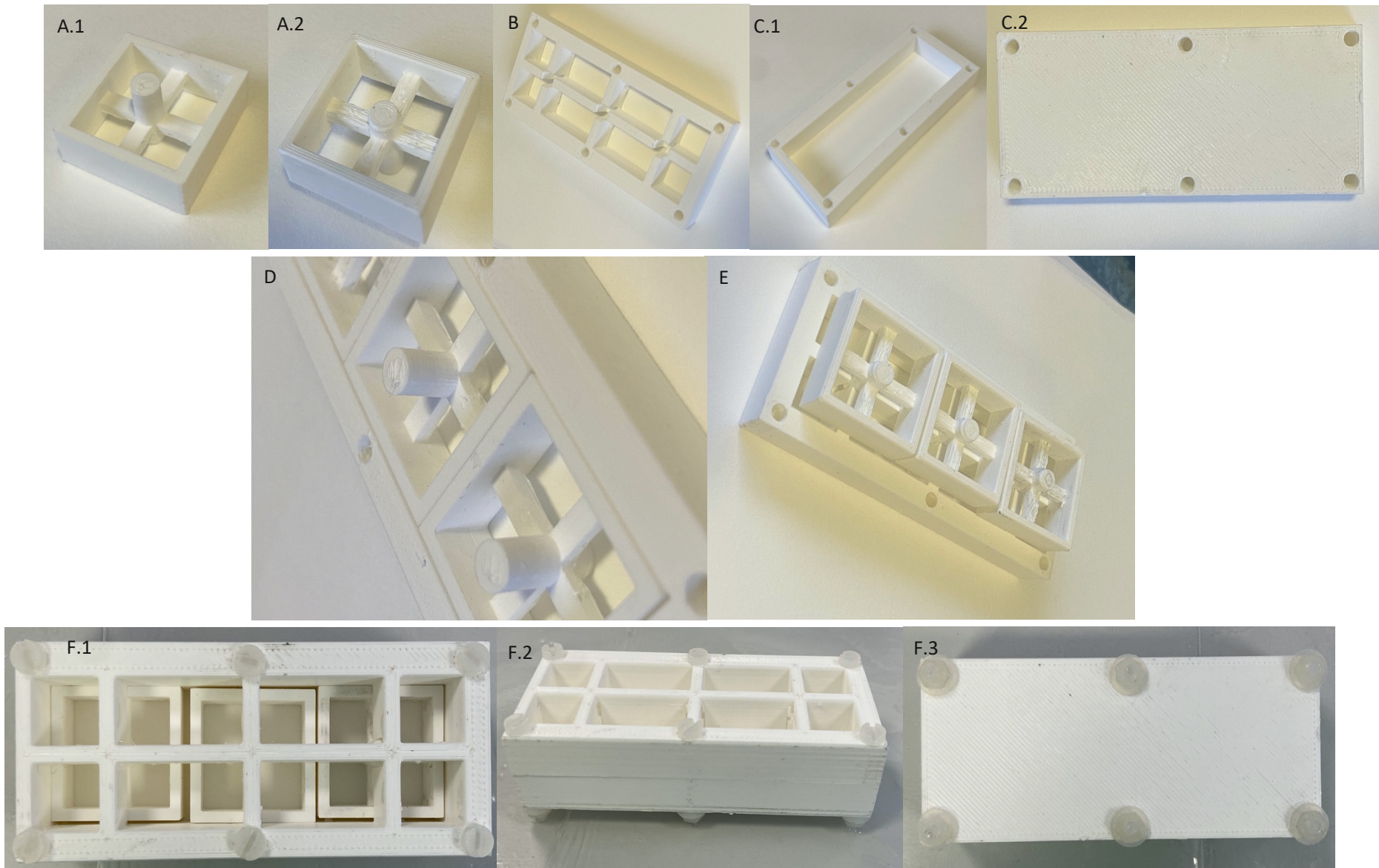


Figure 5.6 Images of components of 3D printed template unit

The 3D printed components of the template unit are as follows: A.1 the orthogonal view of the template, showing  $f$ , the longer section of the cylinder with A.2 highlighting  $s$ , the shorter part. B depicts the holder, which  $f$  fits into. C.1 is the top side of the base and C.2 is the underside. D shows the three templates fitted into the base, with  $l$  being visible. E illustrates the three templates in the holder, with  $s$  visible. F.1, F.2 and F.3 show the top, orthogonal and under view, respectively, of the template unit assembled with washer, screws and nuts.

### 5.2.3 RPA studies

Once the device was made, RPA studies could be conducted as described in the Materials and Methods section.

The data was handled in two distinct ways. Firstly, a log calibration curve was calculated to verify linearity and then subsequently, a sigmoidal semi-log dose response curve was done to highlight the LOD.

The sigmoidal semi-log dose response curve was employed by this research group for all previous studies and so, was maintained for this analysis. The goal of the entire study is to create a test that is qualitative, that is, gives a Yes/No response for the presence of VIM template. Therefore, the LOD is the most important validation parameter of this research.

The LOD is assumed to be the value above the blank measurement denoting the threshold from which the assay can detect the presence or absence of an analyte [85]. The simple model for determining the LOD relies on calculating the mean measurements and standard deviation from blank replicates. The standard deviation is multiplied by a factor of 2-10 and added to mean of the replicates. For this study the LOD was calculated as the mean of the no-template control (NTC) + 3 (STDEV) of the blank [85].

A semi-log dose-response curve was generated using Origin pro (OriginLab, 2021), coefficient of variation (R squared) and standard deviations were calculated for the curve. The limit of detection (LOD) for the curve was calculated as the sum of the mean absorbance of the no template controls (NTCs)/ blank plus three times the standard deviation.

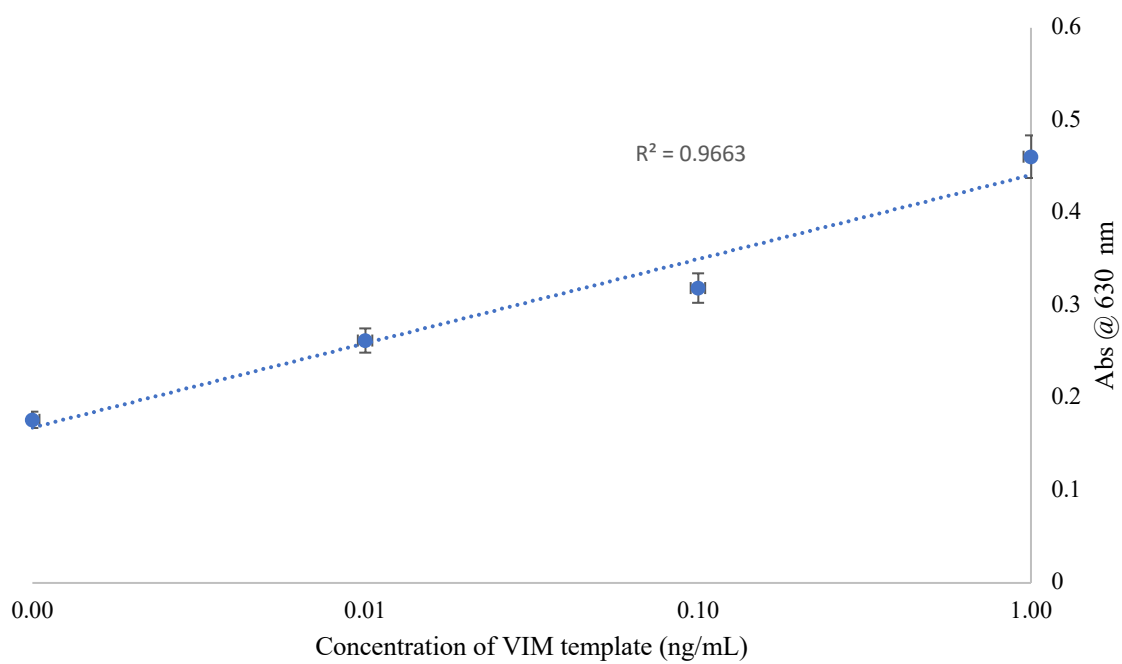


Fig. 5.7 The linearity graph for VIM detection using paper-based device with error bars denoting the standard deviations.

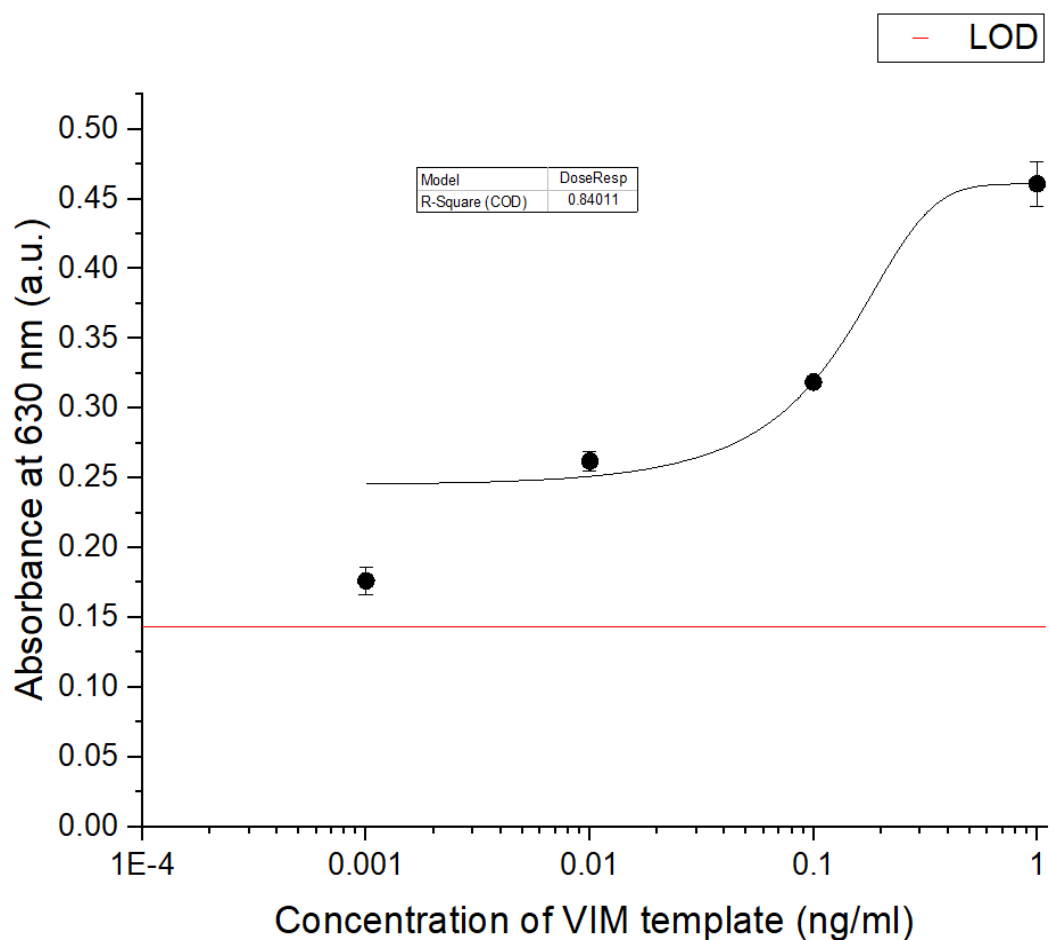


Fig. 5.8 A sigmoidal dose response curve for VIM detection using paper-based device. The red line denotes the LOD with error bars depicting the standard deviations.

The log curve showed great linearity for the method with a  $R^2$  of 0.9663. The most pertinent information for this study, the LOD, could not be explicitly determined. As shown above, the curve does not intersect with the red line which denotes the LOD. This simply means that lower concentrations of VIM template should be tested in order to determine the LOD of this assay. From this proof-of concept study, a VIM template concentration of at least  $0.001 \text{ ngmL}^{-1}$  can be determined, which is very promising for future developments.

### 5.3 Conclusion

This study served as a proof- of- principle study in the establishment of a more intricate device and proved that RPA could in fact be conducted on a paper platform. Sol gel was also confirmed as a suitable hydrophobic material for the creation of boundaries and the use of a 3D-printed

template unit was successful for the patterning step in the development of the paper-based microfluidic.

#### 5.4 Future work

Transferring the sol gel onto a device that can allow for greater ease of patterning would be advantageous. The Epson EcoTank ET-2811 printer, for example, features cartridges which can be filled with inks without the need for injections as attempted before in the investigations. This will allow for printing of the device in a similar way to the wax printing and has great promise for more detailed designs. Additionally, lower VIM template concentrations can be assessed as it seems the assay on paper has potential for much lower concentrations.

## 6. ABBREVIATIONS

%RSD	Percentage relative standard deviation
Abs	Absorbance
AMR	Antimicrobial resistance
APIs	active pharmaceutical ingredients
CE-UV	Capillary electrophoresis with ultraviolet detection
dL	deciliter
DNBA	3,5-dinitrobenzoic acid
FDM	Fuse Deposition Modelling
GC-MS	Gas chromatography-mass spectrometry
GD	Gas diffusion
gL <sup>-1</sup>	Grams per liter
h	Hours

HPLC High performance  
liquid chromatography

ICP-  
MS Inductively coupled  
plasma mass  
spectrometry

LC-  
MSMS Liquid chromatography  
coupled with tandem  
mass spectrometric  
detection

LFA lateral flow assay

LLOQ Lower limit of  
quantification

LOD Limit of detection

mg milligrams

mL milliliters

$\mu$ L microliter

mM millimolar

$\mu$ PAD paper-based  
microfluidic analytical  
devices

MSQ Methylsilsesquioxane

MTMS	Trimethoxymethylsilane
ng	nanogram
nm	nanometer
NR	Nessler's reagent
NTC	no-template control
PA	Picric Acid
PBS	Phosphate-buffered saline
PCP	phencyclidine
PCR	polymerase chain reaction
PDMS	polydimethylsiloxane
PLA	Polylactic Acid
PMI	Post-mortem Interval
POCT	point-of-care test
PONT	point-of-need test
PTFE	polytetrafluoroethylene
RGB	Red, Green, Blue

RPA	recombinase polymerase amplification
RTP	Room temperature and pressure
s	Seconds
SERS	Surface-enhanced Raman spectroscopy
STDEV	Standard deviation
TMB	3, 3', 5, 5'- tetramethylbenzidine
ULOQ	Upper limit of quantification
VH	vitreous humour
VIM	Verona integron- encoded metallo- $\beta$ - lactamase
WHO	World Health Organisation

## 7. REFERENCES

1. Musile, G., et al., *Paper-based microfluidic devices: On-site tools for crime scene investigation*. TrAC Trends in Analytical Chemistry, 2021. **143**: p. 116406.
2. Musile, G., et al., *The development of paper microfluidic devices for presumptive drug detection*. Analytical Methods, 2015. **7**(19): p. 8025-8033.
3. Boehle, K.E., et al., *based enzyme competition assay for detecting falsified  $\beta$ -lactam antibiotics*. ACS sensors, 2018. **3**(7): p. 1299-1307.
4. Green, M.D., et al., *A colorimetric field method to assess the authenticity of drugs sold as the antimalarial artesunate*. Journal of pharmaceutical and biomedical analysis, 2000. **24**(1): p. 65-70.
5. Pratiwi, R., et al., *Design and optimization of colorimetric paper-based analytical device for rapid detection of allopurinol in herbal medicine*. International journal of analytical chemistry, 2019. **2019**.
6. Cromartie, R.L., et al., *Development of a microfluidic device ( $\mu$ PADs) for forensic serological analysis*. Analytical Methods, 2019. **11**(5): p. 587-595.
7. Buring, S., et al., *Microfluidic Paper-based Analytical Device for Quantification of Lead Using Reaction Band-length for Identification of Bullet Hole and Its Potential for Estimating Firing Distance*. Anal Sci, 2018. **34**(1): p. 83-89.
8. Musile, G., et al., *Thanatochemistry at the crime scene: a microfluidic paper-based device for ammonium analysis in the vitreous humor*. Analytica Chimica Acta, 2019. **1083**: p. 150-156.
9. Azuaje-Hualde, E., et al., *Naked eye Y amelogenin gene fragment detection using DNAzymes on a paper-based device*. Analytica Chimica Acta, 2020. **1123**: p. 1-8.
10. Pesenti, A., et al., *Coupling paper-based microfluidics and lab on a chip technologies for confirmatory analysis of trinitro aromatic explosives*. Analytical Chemistry, 2014. **86**(10): p. 4707-4714.
11. Pardasani, D., et al.,  *$\mu$ -PADs for detection of chemical warfare agents*. Analyst, 2012. **137**(23): p. 5648-5653.
12. Mabey, D., et al., *Diagnostics for the developing world*. Nature Reviews Microbiology, 2004. **2**(3): p. 231-240.
13. Land, K.J., *based Diagnostics: Current Status and Future Applications*. 2018: Springer.
14. Merrin, J., *Frontiers in Microfluidics, a Teaching Resource Review*. Bioengineering (Basel, Switzerland), 2019. **6**(4): p. 109.
15. Martinez, A.W., et al., *Patterned paper as a platform for inexpensive, low-volume, portable bioassays*. Angewandte Chemie International Edition, 2007. **46**(8): p. 1318-1320.
16. Auhorn, W.J., *Chemical additives for papermaking - High performance at low levels of addition guarantees progress*. Wochenblatt fuer Papierfabrikation, 1999. **127**(23-24): p. 1558-1572.
17. Lv, Y., T. Tan, and F. Svec, *Molecular imprinting of proteins in polymers attached to the surface of nanomaterials for selective recognition of biomacromolecules*. Biotechnology advances, 2013. **31**(8): p. 1172-1186.
18. Saylan, Y., E. Tamahkar, and A. Denizli, *Recognition of lysozyme using surface imprinted bacterial cellulose nanofibers*. Journal of Biomaterials science, Polymer edition, 2017. **28**(16): p. 1950-1965.
19. Liu, J., D. Mazumdar, and Y. Lu, *A simple and sensitive "dipstick" test in serum based on lateral flow separation of aptamer-linked nanostructures*. Angewandte Chemie, 2006. **118**(47): p. 8123-8127.
20. Toh, S.Y., et al., *Aptamers as a replacement for antibodies in enzyme-linked immunosorbent assay*. Biosensors and bioelectronics, 2015. **64**: p. 392-403.
21. Wilson, D.S. and J.W. Szostak, *In vitro selection of functional nucleic acids*. Annual review of biochemistry, 1999. **68**(1): p. 611-647.

22. Carrell, C., et al., *Beyond the lateral flow assay: A review of paper-based microfluidics*. *Microelectronic Engineering*, 2019. **206**: p. 45-54.
23. Martinez, A.W., et al., *Simple telemedicine for developing regions: Camera phones and paper-based microfluidic devices for real-time, off-site diagnosis*. *Analytical Chemistry*, 2008. **80**(10): p. 3699-3707.
24. Lu, R., et al., *Rapid prototyping of paper-based microfluidics with wax for low-cost, portable bioassay*. *Electrophoresis*, 2009. **30**(9): p. 1497-1500.
25. Carrilho, E., A.W. Martinez, and G.M. Whitesides, *Understanding wax printing: A simple micropatterning process for paper-based microfluidics*. *Analytical Chemistry*, 2009. **81**(16): p. 7091-7095.
26. Li, X., D.R. Ballerini, and W. Shen, *A perspective on paper-based microfluidics: Current status and future trends*. *Biomicrofluidics*, 2012. **6**(1).
27. Jahanshahi-Anbuhi, S., et al., *Creating fast flow channels in paper fluidic devices to control timing of sequential reactions*. *Lab on a Chip*, 2012. **12**(23): p. 5079-5085.
28. Wang, J., et al., *Hydrophobic sol-gel channel patterning strategies for paper-based microfluidics*. *Lab on a Chip*, 2014. **14**(4): p. 691-695.
29. Qu, L.L., et al., *Batch fabrication of disposable screen printed SERS arrays*. *Lab on a Chip*, 2012. **12**(5): p. 876-881.
30. Wang, H., et al., *Paper spray for direct analysis of complex mixtures using mass spectrometry*. *Angewandte Chemie - International Edition*, 2010. **49**(5): p. 877-880.
31. Madea, B. and F. Musshoff, *Postmortem biochemistry*. *Forensic science international*, 2007. **165**(2-3): p. 165-171.
32. Tagliaro, F., et al., *Potassium concentration differences in the vitreous humour from the two eyes revisited by microanalysis with capillary electrophoresis*. *Journal of Chromatography A*, 2001. **924**(1-2): p. 493-498.
33. Gottardo, R., et al., *A new method for the determination of ammonium in the vitreous humour based on capillary electrophoresis and its preliminary application in thanatochemistry*. *Clinical Chemistry and Laboratory Medicine (CCLM)*, 2019. **57**(4): p. 504-509.
34. Thierauf, A., F. Musshoff, and B. Madea, *Post-mortem biochemical investigations of vitreous humor*. *Forensic science international*, 2009. **192**(1-3): p. 78-82.
35. Farmer, J., et al., *Magnesium, potassium, sodium and calcium in post-mortem vitreous humour from humans*. *Forensic science international*, 1985. **27**(1): p. 1-13.
36. Santos Junior, J.C., et al., *Metals and (metallo) proteins identification in vitreous humor focusing on post-mortem biochemistry*. *Metallomics*, 2014. **6**(10): p. 1801-1807.
37. Peclat, C., P. Picotte, and F. Jobin, *The use of vitreous humor levels of glucose, lactic acid and blood levels of acetone to establish antemortem hyperglycemia in diabetics*. *Forensic science international*, 1994. **65**(1): p. 1-6.
38. Tagliaro, F., et al., *Capillary zone electrophoresis of potassium in human vitreous humour: validation of a new method*. *Journal of Chromatography B: Biomedical Sciences and Applications*, 1999. **733**(1-2): p. 273-279.
39. Lendoiro, E., et al., *Applications of Tandem Mass Spectrometry (LC-MSMS) in estimating the post-mortem interval using the biochemistry of the vitreous humour*. *Forensic science international*, 2012. **223**(1-3): p. 160-164.
40. Van Den Oever, R., *Post-mortem vitreous ammonium concentrations in estimating the time of death*. *Zeitschrift für Rechtsmedizin*, 1978. **80**(4): p. 259-263.
41. Henssge, C. and B. Madea, *Estimation of the time since death in the early post-mortem period*. *Forensic science international*, 2004. **144**(2-3): p. 167-175.
42. Garcia, P.T., et al., *Paper-based microfluidic devices on the crime scene: A simple tool for rapid estimation of post-mortem interval using vitreous humour*. *Analytica Chimica Acta*, 2017. **974**: p. 69-74.

43. Hadland, S.E. and S. Levy, *Objective Testing: Urine and Other Drug Tests*. Child Adolesc Psychiatr Clin N Am, 2016. **25**(3): p. 549-65.
44. Darwish, I.A., *Immunoassay Methods and their Applications in Pharmaceutical Analysis: Basic Methodology and Recent Advances*. International journal of biomedical science : IJBS, 2006. **2**(3): p. 217-235.
45. Jacobs, R.M., et al., *Effects of interferents on the kinetic Jaffé reaction and an enzymatic colorimetric test for serum creatinine concentration determination in cats, cows, dogs and horses*. Canadian journal of veterinary research, 1991. **55**(2): p. 150.
46. Yao, T. and K. Kotegawa, *Simultaneous flow-injection assay of creatinine and creatine in serum by the combined use of a 16-way switching valve, some specific enzyme reactors and a highly selective hydrogen peroxide electrode*. Analytica Chimica Acta, 2002. **462**(2): p. 283-291.
47. Hewavitharana, A.K. and H.L. Bruce, *Simultaneous liquid chromatographic determination of creatinine and pseudouridine in bovine urine and the effect of sample pH on the analysis*. Journal of agricultural and food chemistry, 2003. **51**(17): p. 4861-4865.
48. Jen, J.-F., S.-L. Hsiao, and K.-H. Liu, *Simultaneous determination of uric acid and creatinine in urine by an eco-friendly solvent-free high performance liquid chromatographic method*. Talanta, 2002. **58**(4): p. 711-717.
49. Tsikas, D., A. Wolf, and J.C. Frölich, *Simplified HPLC method for urinary and circulating creatinine*. Clinical Chemistry, 2004. **50**(1): p. 201-203.
50. Patel, C. and R. George, *Liquid chromatographic determination of creatinine in serum and urine*. Analytical chemistry, 1981. **53**(4): p. 734-735.
51. Marsilio, R., et al., *Rapid determination of creatinine in serum and urine by ion-pair high-performance liquid chromatography*. International Journal of Clinical and Laboratory Research, 1999. **29**(3): p. 103.
52. Paroni, R., et al., *Determination of creatinine in serum and urine by a rapid liquid-chromatographic method*. Clinical chemistry, 1990. **36**(6): p. 830-836.
53. Jia, L., et al., *The determination of creatinine in human urine by capillary zone electrophoresis with photodiode array detection*. Journal of liquid chromatography & related technologies, 1998. **21**(7): p. 965-977.
54. Shi, H., Y. Ma, and Y. Ma, *A simple and fast method to determine and quantify urinary creatinine*. Analytica chimica acta, 1995. **312**(1): p. 79-83.
55. Zinellu, A., et al., *Assay for the simultaneous determination of guanidinoacetic acid, creatinine and creatine in plasma and urine by capillary electrophoresis UV-detection*. Journal of separation science, 2006. **29**(5): p. 704-708.
56. Ruiz-Jiménez, J., J.M. Mata-Granados, and M.D. Luque de Castro, *On-line automatic SPE-CE coupling for the determination of biological markers in urine*. Electrophoresis, 2007. **28**(5): p. 789-798.
57. Felitsyn, N.M., et al., *Liquid chromatography–tandem mass spectrometry method for the simultaneous determination of  $\delta$ -ALA, tyrosine and creatinine in biological fluids*. Clinica chimica acta, 2004. **350**(1-2): p. 219-230.
58. Takahashi, N., et al., *Tandem mass spectrometry measurements of creatinine in mouse plasma and urine for determining glomerular filtration rate*. Kidney international, 2007. **71**(3): p. 266-271.
59. Park, E.-K., et al., *Creatinine Measurements in 24 h Urine by Liquid Chromatography– Tandem Mass Spectrometry*. Journal of agricultural and food chemistry, 2008. **56**(2): p. 333-336.
60. Hou, H., et al., *LC-MS-MS measurements of urinary creatinine and the application of creatinine normalization technique on cotinine in smokers' 24 hour urine*. Journal of analytical methods in chemistry, 2012. **2012**.
61. Jaffé, M., *Ueber den Niederschlag, welchen Pikrinsäure in normalem Harn erzeugt und über eine neue Reaction des Kreatinins*. Zeitschrift für physiologische Chemie, 1886. **10**(5): p. 391-400.

62. Folin, O. and H. Wu, *A system of blood analysis Supplement I. A simplified and improved method for determination of sugar*. Journal of Biological Chemistry, 1920. **41**(3): p. 367-374.
63. Peake, M. and M. Whiting, *Measurement of serum creatinine—current status and future goals*. Clinical biochemist reviews, 2006. **27**(4): p. 173.
64. Langley, W.D. and M. Evans, *The determination of creatinine with sodium 3, 5-dinitrobenzoate*. Journal of Biological Chemistry, 1936. **115**(1): p. 333-341.
65. Bollinger, A., *Colorimetric determination of creatinine in urine and blood with 3, 5-dinitrobenzoic acid*. Med. J. Aust, 1936. **2**: p. 818.
66. Benedict, S.R. and J.A. Behre, *Some applications of a new color reaction for creatinine*. Journal of biological chemistry, 1936. **114**(2): p. 515-532.
67. Nessler, J., *On the behavior of iodide of mercury to ammonia, and a new reaction for ammonia*. J. Prakt. Chem., 1856. **14**: p. 445-453.
68. Sarkar, P.B. and N.N. Ghosh, *Studies on nessler's reagent part I*. Analytica Chimica Acta, 1955. **13**: p. 195-199.
69. Cate, D.M., et al., *Recent developments in paper-based microfluidic devices*. Analytical chemistry, 2015. **87**(1): p. 19-41.
70. Sununta, S., et al., *Microfluidic Paper-based Analytical Devices for Determination of Creatinine in Urine Samples*. Analytical Sciences, 2018. **34**(1): p. 109-113.
71. Cone, E.J., et al., *Normalization of Urinary Drug Concentrations with Specific Gravity and Creatinine*. Journal of Analytical Toxicology, 2009. **33**(1): p. 1-7.
72. Sarigul, N., F. Korkmaz, and İ. Kurultak, *A New Artificial Urine Protocol to Better Imitate Human Urine*. Scientific Reports, 2019. **9**(1): p. 20159.
73. Riley, J.C., *Estimates of Regional and Global Life Expectancy, 1800–2001*. Population and Development Review, 2005. **31**(3): p. 537-543.
74. CDC, *Leading Causes of Death, 1900-1998* 1999.
75. Colebrook, L. and M. Kenny, *Treatment of human puerperal infections, and of experimental infections in mice, with prontosil*. The Lancet, 1936. **227**(5884): p. 1279-1281.
76. Abraham, E.P. and E. Chain, *An Enzyme from Bacteria able to Destroy Penicillin*. Nature, 1940. **146**(3713): p. 837-837.
77. Giske, C.G., et al., *Establishing clonal relationships between VIM-1-like metallo- $\beta$ -lactamase-producing Pseudomonas aeruginosa strains from four European countries by multilocus sequence typing*. Journal of clinical microbiology, 2006. **44**(12): p. 4309-4315.
78. Garibyan, L. and N. Avashia, *Polymerase chain reaction*. J Invest Dermatol, 2013. **133**(3): p. 1-4.
79. Mullis, K., et al. *Specific enzymatic amplification of DNA in vitro: the polymerase chain reaction*. in *Cold Spring Harbor symposia on quantitative biology*. 1986. Cold Spring Harbor Laboratory Press.
80. Crannell, Z., et al., *Multiplexed recombinase polymerase amplification assay to detect intestinal protozoa*. Analytical chemistry, 2016. **88**(3): p. 1610-1616.
81. Crannell, Z.A., et al., *Nucleic acid test to diagnose cryptosporidiosis: lab assessment in animal and patient specimens*. Analytical chemistry, 2014. **86**(5): p. 2565-2571.
82. Piepenburg, O., et al., *DNA detection using recombination proteins*. PLoS biology, 2006. **4**(7): p. e204.
83. Van Reenen, A., et al., *Integrated lab-on-chip biosensing systems based on magnetic particle actuation—a comprehensive review*. Lab on a Chip, 2014. **14**(12): p. 1966-1986.
84. Nie, J., et al., *Low-cost fabrication of paper-based microfluidic devices by one-step plotting*. Analytical Chemistry, 2012. **84**(15): p. 6331-6335.
85. Armbruster, D.A. and T. Pry, *Limit of blank, limit of detection and limit of quantitation*. The Clinical biochemist. Reviews, 2008. **29 Suppl 1**(Suppl 1): p. S49-S52.

## 8. APPENDICES

### 8.1 Appendix I. $\text{NH}_4^+$ in vitreous humour

#### 8.1.1 List of vitreous humour samples used in the study

*Table 8.1: List of vitreous humour samples with the corresponding ammonium concentrations acquired for the CE-UV method as well as the determined concentrations using GD and  $\mu\text{PAD}$  methods.*

<b>VH sample #</b>	<b><math>[\text{NH}_4^+]/\text{mM}</math> CE-UV method</b>	<b><math>[\text{NH}_4^+]/\text{mM}</math> GD method</b>	<b><math>[\text{NH}_4^+]/\text{mM}</math> <math>\mu\text{PAD}</math> method</b>
1	2.25	2.77	1.07
2	3.76	2.70	1.09
3	0.34	0.91	0.32
4	0.26	0.41	0.29
5	1.28	1.41	1.15
6	0.94	1.30	0.77
7	1.01	0.84	0.96
8	0.76	1.14	0.80
9	0.69	0.87	0.54
10	0.32	0.71	0.38
11	0.47	0.86	0.38
12	0.45	0.84	0.47
13	0.76	0.96	0.59
14	0.62	0.76	0.59
15	0.85	0.94	0.78
16	1.06	1.38	0.90
17	0.2	0.79	0.40
18	0.68	1.18	0.41
19	1.5	1.34	1.14
20	0.84	1.14	1.13
21	1.15	1.39	1.35
22	1.01	1.43	0.93
23	0.99	1.22	1.04
24	0.61	0.87	0.57
25	2.34	2.26	1.07
26	1.93	2.87	1.00
27	2.09	2.56	1.69

### 8.1.2 Reproducibility studies for GD and $\mu$ PAD methods

Table 8.2: Reproducibility studies for  $\mu$ PAD method

	Calibrators levels, mM				
	0.50	0.75	1.00	1.25	1.50
<b>Precision within-run, %RSD</b>					
<i>Day 1 (n=3)</i>	1.0	8.9	1.6	4.8	4.6
<i>Day 2 (n=3)</i>	13.2	9.2	13.1	2.5	11.4
<i>Day 3 (n=3)</i>	4.3	6.5	11.3	9.1	3.8
<i>Day 4 (n=3)</i>	12.8	8.1	5.0	3.9	7.0
<i>Day 5 (n=3)</i>	12.8	6.5	11.3	9.1	3.8
<i>Day 6 (n=3)</i>	11.9	11.6	7.9	6.2	11.11
<b>Precision between runs, %RSD</b>					
<i>n=18</i>	9.3	8.5	8.3	5.9	7.0
<b>Accuracy within-run, %RSD</b>					
<i>Day 1 (n=3)</i>	106.3	88.8	93.2	92.1	85.9
<i>Day 2 (n=3)</i>	114.0	108.1	103.2	90.9	90.6
<i>Day 3 (n=3)</i>	95.4	103.1	103.4	96.5	100.7
<i>Day 4 (n=3)</i>	97.6	104.2	100.9	115.4	104.6
<i>Day 5 (n=3)</i>	97.6	103.1	103.4	96.5	100.7
<i>Day 6 (n=3)</i>	115.3	119.9	107.7	100.6	93.6
<b>Accuracy between runs, %RSD</b>					
<i>n=18</i>	104.4	104.5	101.9	98.7	96.01

Table 8.3: Reproducibility studies for GD method

	Calibrators levels, mM				
	0.3125	0.50	0.75	1.00	1.5
<b>Precision within-run, %RSD</b>					
<i>Day 1 (n=3)</i>	10.2	6.5	2.7	2.9	6.0
<i>Day 2 (n=3)</i>	3.1	6.9	5.8	6.1	1.7
<i>Day 3 (n=3)</i>	15.7	6.5	9.9	10.0	1.0
<i>Day 4 (n=3)</i>	6.7	11.8	4.9	3.7	2.8
<i>Day 5 (n=3)</i>	12.0	5.5	10.8	7.1	6.6
<i>Day 6 (n=3)</i>	8.0	5.4	9.9	5.5	3.6
<b>Precision between runs, %RSD</b>					
<i>n=18</i>	9.3	7.1	7.3	5.9	3.6
<b>Accuracy within-run, %RSD</b>					
<i>Day 1 (n=3)</i>	98.6	85.0	108.5	95.3	110.2
<i>Day 2 (n=3)</i>	91.7	90.7	109.4	111.9	94.2
<i>Day 3 (n=3)</i>	88.3	85.0	100.7	109.9	86.7
<i>Day 4 (n=3)</i>	87.0	99.9	111.3	94.2	92.8
<i>Day 5 (n=3)</i>	96.2	102.6	104.8	96.8	85.1
<i>Day 6 (n=3)</i>	102.0	91.0	106.3	106.3	85.8
<b>Accuracy between runs, %RSD</b>					
<i>n=18</i>	94.0	92.4	106.8	102.4	92.4

## 8.2 Appendix II. Creatinine in urine

### 8.2.1 List of urine samples used in the study

*Table 8.4: List of urine samples with the corresponding creatinine concentrations acquired for the immunoassay method as well as the determined concentrations using NR, PA and DNBA.*

Urine sample #	Immunoassay method	RGB Distance			Calculated creatinine concentrations/ gL <sup>-1</sup>		
	[Creatinine]/ gL <sup>-1</sup>	NR	PA	DNBA	NR	PA	DNBA
1	0.103	121	54	157	0.351	0.109	0.539
2	0.077	107	46	144	0.308	0.082	0.490
3	0.031	92	34	115	0.262	0.040	0.381
4	0.068	144	53	149	0.422	0.106	0.509
5	0.052	110	37	120	0.317	0.051	0.400
6	0.133	163	72	183	0.480	0.172	0.637
7	0.108	138	50	161	0.403	0.096	0.554
8	0.046	128	43	128	0.373	0.071	0.430
9	0.025	107	30	93	0.308	0.026	0.298
10	0.135	134	64	176	0.391	0.144	0.610
11	0.076	138	66	154	0.403	0.151	0.527
12	0.057	116	44	109	0.336	0.075	0.358
13	0.101	134	37	161	0.391	0.051	0.554

## 8.2.2 Reproducibility studies for the reagents used in the study

Table 8.5: Reproducibility studies for creatinine studies using NR

	Calibrators levels, gL <sup>-1</sup>				
	0.02	0.06	0.10	0.15	0.20
<b>Precision within-run, %RSD</b>					
<i>Day 1 (n=3)</i>	5.6	6.1	3.2	5.1	4.2
<i>Day 2 (n=3)</i>	3.1	6.9	4.2	7.5	2.3
<i>Day 3 (n=3)</i>	12.3	5.4	8.9	11.2	1.0
<i>Day 4 (n=3)</i>	6.7	8.1	4.9	3.6	2.9
<i>Day 5 (n=3)</i>	12.0	10.5	9.8	7.9	6.6
<i>Day 6 (n=3)</i>	8.0	4.5	5.9	5.5	3.9
<b>Precision between runs, %RSD</b>					
<i>n=18</i>	7.0	6.9	6.2	6.8	3.5
<b>Accuracy within-run, %RSD</b>					
<i>Day 1 (n=3)</i>	98.6	85.8	103.5	93.5	101.3
<i>Day 2 (n=3)</i>	95.2	91.3	102.1	110.2	95.3
<i>Day 3 (n=3)</i>	88.3	85.0	100.7	108.1	87.6
<i>Day 4 (n=3)</i>	89.0	100.0	111.3	94.2	92.8
<i>Day 5 (n=3)</i>	98.2	103.2	98.6	98.6	90.5
<i>Day 6 (n=3)</i>	103.1	95.6	105.9	106.1	95.8
<b>Accuracy between runs, %RSD</b>					
<i>n=18</i>	95.4	93.5	103.7	101.8	93.9

Table 8.6: Reproducibility studies for creatinine studies using PA

	Calibrators levels, gL <sup>-1</sup>				
	0.02	0.06	0.10	0.15	0.20
<b>Precision within-run, %RSD</b>					
<i>Day 1 (n=3)</i>	5.4	3.1	8.5	5.2	4.2
<i>Day 2 (n=3)</i>	2.3	9.5	10.2	7.1	3.5
<i>Day 3 (n=3)</i>	1.2	5.4	8.9	1.8	1.0
<i>Day 4 (n=3)</i>	5.6	8.3	4.9	3.6	3.1
<i>Day 5 (n=3)</i>	7.2	1.5	9.8	7.9	4.6
<i>Day 6 (n=3)</i>	8.0	3.5	5.9	6.8	3.9
<b>Precision between runs, %RSD</b>					
<i>n=18</i>	5.0	5.2	8.0	5.4	3.4
<b>Accuracy within-run, %RSD</b>					
<i>Day 1 (n=3)</i>	102.6	98.1	101.0	93.3	102.4
<i>Day 2 (n=3)</i>	95.2	95.3	108.2	90.2	95.3
<i>Day 3 (n=3)</i>	86.3	85.6	102.7	100.1	88.7
<i>Day 4 (n=3)</i>	89.2	101.8	95.3	94.2	93.2
<i>Day 5 (n=3)</i>	98.2	105.6	98.6	96.6	91.5
<i>Day 6 (n=3)</i>	101.8	96.6	105.3	90.1	95.8
<b>Accuracy between runs, %RSD</b>					
<i>n=18</i>	95.6	97.2	101.9	94.1	94.5

Table 8.7: Reproducibility studies for creatinine studies using DNBA

	Calibrators levels, gL <sup>-1</sup>				
	0.02	0.06	0.10	0.15	0.20
<b>Precision within-run, %RSD</b>					
<i>Day 1 (n=3)</i>	6.3	9.4	3.3	7.4	4.2
<i>Day 2 (n=3)</i>	3.1	6.1	4.3	7.2	2.8
<i>Day 3 (n=3)</i>	1.6	5.4	9.5	1.3	6.3
<i>Day 4 (n=3)</i>	6.8	8.0	10.1	3.9	2.9
<i>Day 5 (n=3)</i>	12.1	5.3	9.3	8.9	6.8
<i>Day 6 (n=3)</i>	8.5	1.5	5.9	5.8	3.0
<b>Precision between runs, %RSD</b>					
<i>n=18</i>	6.4	6.0	7.1	5.8	4.3
<b>Accuracy within-run, %RSD</b>					
<i>Day 1 (n=3)</i>	108.2	89.9	102.5	103.3	101.3
<i>Day 2 (n=3)</i>	98.2	98.3	100.1	101.2	95.3
<i>Day 3 (n=3)</i>	88.9	95.0	90.4	88.1	97.9
<i>Day 4 (n=3)</i>	89.0	90.0	101.6	104.4	88.6
<i>Day 5 (n=3)</i>	98.2	103.2	98.6	98.6	95.0
<i>Day 6 (n=3)</i>	100.1	98.9	106.9	96.1	95.8
<b>Accuracy between runs, %RSD</b>					
<i>n=18</i>	97.1	95.9	100.0	98.6	95.7

## 8.3 Appendix III. RPA Studies

### 8.3.1 Schematic of Recombinase Polymerase Amplification

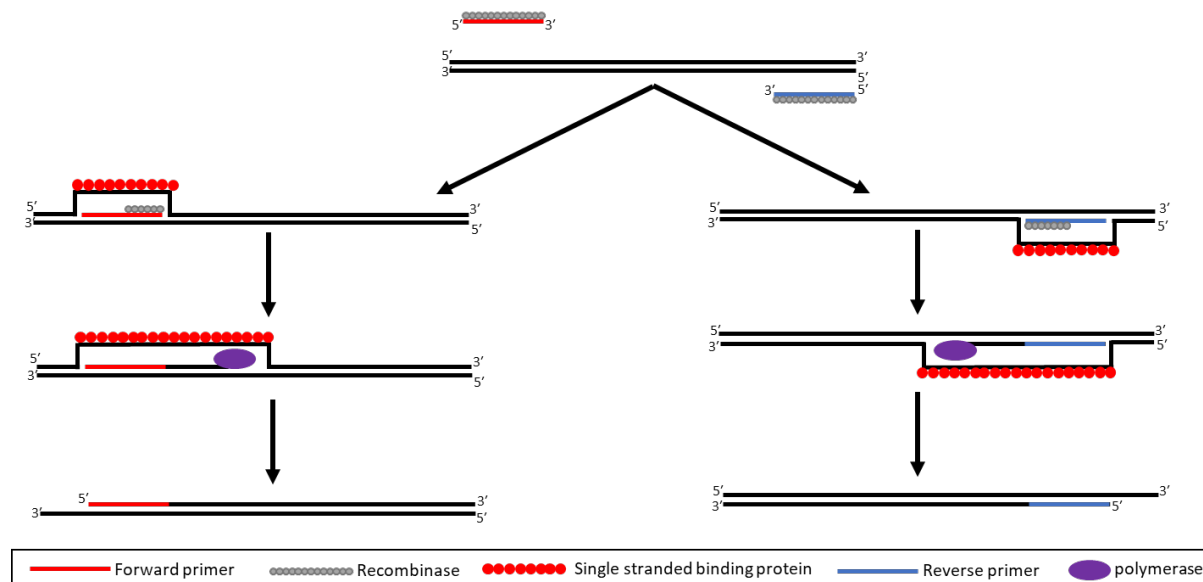


Figure 8.1 Schematic of Recombinase polymerase amplification.

The recombinase in grey interacts with the forward (red) and reverse (blue) primer to scan down the DNA for a homologous sequence once found recombinase facilitates strand exchange and single stranded binding proteins (red circles) interact with the opposing strand. BSU polymerase (purple) is recruited to the 3' of the primer and initiated DNA synthesis. These steps are repeated for the duration of the reaction. Based on figures from [82].

### 8.3.2 Full list of Chemicals

Attenuated *E.coli* Top10 cells, PureYield plasmid midiprep system, and 100  $\mu$ M dNTP were purchased from Promega. Synthetic plasmids containing *bla*<sub>VIM-2</sub>, and custom DNA oligonucleotides were all purchased from Integrated DNA Technologies. Biotin-TEG single stranded oligonucleotides (capture probes), Biotin-TEG forward primers, and 5'HRP conjugated single stranded oligonucleotides (reporter probes) were purchased from Biomers.net. UltraPure Agarose 1000 and E-gel low-range quantitative DNA ladder were purchased from Invitrogen. 10,000x GelRed nucleic acid stain was purchased from Biotium. Nucleic acid loading buffer and EZ load 20 bp molecular ruler were provided by Bio-Rad. TwistAmp basic kit and TwistAmp Liquid basic kit were purchased from TwistDX. Pierce

High binding streptavidin coated plates were provided by Thermo Fischer Scientific. KPL sureblueTMB (3, 3', 5, 5'-tetramethylbenzidine) microwell peroxidase substrate was purchased from Seracare. Luria-Bertani (LB) broth low salt granulated was purchased from Melford. Tween 20 was purchased from Sigma. Within this project PBS was made to pH 7.2 with 2.7 mM KCl, 1.5 mM KH<sub>2</sub>PO<sub>4</sub>, 8 mM Na<sub>2</sub>HPO<sub>4</sub>, 138 mM NaCl. Streptavidin Mono Magnetic beads, 1 µm were bought from Ocean Nanotech.

### 8.3.3 Functionalising/ Priming of Magnetic beads with VIM Biotinylated Forward primer

Two- 500 µL aliquots of streptavidin coated magnetic beads are primed. Firstly, the aliquots are added to low binding capacity tubes and washed three times using 1 mL of 1x PBS + 0.05% Tween buffer. To one aliquot, 7.9 µL of 100 µM VIM 5' Biotin Fwd primer is added and to the second (uncoated beads which serve as the control) 7.9 µL of water is added. One mL of 1x PBS + 0.05% Tween buffer was added and the tubes placed on a carousel for 1 h for the primer to bind. The aliquots were then washed three times with 1x PBS + 0.05% Tween buffer and vortexed. The buffer is removed from the aliquots of beads and resuspended in 250 µL of water.

### 8.3.4 Components of RPA mixture

The master mix was set up according to the TwistAmp® Liquid Basic Kit's instructions:

*Table 7.8: Components and volumes of RPA mixture*

Component	Volume / µL
2x Reaction buffer	25
dNTPs	3.6
Water	4
20x core reaction mix	2.5
10x Probe E-mix	5
Reverse primer	2.4
VIM DNA template	5

30 µL of the master mix was used in the RPA study.

### 8.3.5 Results of RPA studies

Table 8.9: Results from RPA studies

Concentration/ ngmL <sup>-1</sup>	Abs @ 630 nm			Average	STDEV
	1	2	3		
1	0.4429	0.4745	0.4648	0.4607	0.0162
0.1	0.3178	0.3162	0.3221	0.3187	0.0031
0.01	0.2664	0.2654	0.2542	0.262	0.0068
0.001	0.1866	0.1667	0.1755	0.1763	0.0099
NTC	0.123	0.113	0.103	0.113	0.0100
Naked beads	0.0935	0.0834	0.0752		

**LOD:  $0.113 + 3(0.01) = 0.143$**

## 9. ACKNOWLEDGEMENTS

Throughout the writing of this dissertation, I have received a great deal of support and assistance.

I would first like to thank my supervisor, Professor Franco Tagliaro and tutor Dr. Giacomo Musile, whose knowledge was invaluable in formulating the research questions and methodology. Also, for their valuable guidance throughout these three years. You provided me with the tools that I needed to choose the right direction and successfully complete my dissertation.

I would also like to extend my deepest gratitude to all my colleagues from Medicina Legale. To Prof.ssa Federica Bortolotti for her help, assistance and advice through different times of my PhD. To Prof. Elio d Palo, Prof.ssa Rossella Gottardo, Dr. Nadia Porpiglia, Dr. Anna Bertaso, Dr. Francesco Taus, Matilde, Marco and Sara for all their help, support, supervision, teaching, fun days at the laboratory, and friendship. A special thank you to Cova and Ksenia. I will cherish our friendship and adventures together, forever.

I would like to thank Dr Neil Keegan who facilitated my fruitful research abroad placement at Newcastle University during a pandemic. To the lab group Julia, Chris, Terri, Matt and Erin. Thank you for helping and being patient with me as I learned new concepts. And of course, for the amazing conversations.

To my family, the Agards and Goodridges, you have all played a role in who I am today, and I am so grateful to you all. You keep me grounded and make me laugh and remind me of my why. Mummy Sylo, Uncle Matthew, Aunty Angela, Tata, Aunty Hilary, Aunty Ally, JuneJune, Nanan, Tamie, Emo, DeanDean, Yannick, Annie, Adele, Ishy, my Zowé, I love and miss you all. Thank you for shaping me. Thank you, Daddy. To Ron, Sergina and Evni, thank you for standing in as surrogate children during my time away.

To my friends, all of who I love so much, and who have been instrumental in my darkest and happiest of times. I love growing with you. I love evolving with you. I love all our memories

and the many more we will create. Yetta, Twinkle, Reni, Ilsie, Gracie, Lau, Khea, Larry, Peanell, Pixie, Princess, Melanie and Shenice, thank you.

I am appreciative of you all. Thank you.